

Spin-glass phase of cuprates

N. Hasselmann^{1,2}, A. H. Castro Neto³, and C. Morais Smith⁴

¹ *Max-Planck-Institut für Physik komplexer Systeme, Nöthnitzer Str. 38, 01187 Dresden, Germany*

² *Institut für Theoretische Physik, Universität Frankfurt, Robert-Mayer-Str. 8, 60054 Frankfurt, Germany*

³ *Department of Physics, Boston University, 590 Commonwealth Ave, Boston, MA, 02215*

⁴ *Département de Physique, Université de Fribourg, Pérolles, CH-1700 Fribourg, Switzerland.*

(Dated: May 26, 2020)

We investigate a phenomenological model for the spin glass phase of $\text{La}_{2-x}\text{Sr}_x\text{CuO}_4$, in which it is assumed that holes doped into the CuO_2 planes localize near their Sr dopant, where they cause a dipolar frustration of the antiferromagnetic environment. In absence of long-range antiferromagnetic order, the spin system can reduce frustration, and also its free energy, by forming a state with an ordered orientation of the dipole moments, which leads to the appearance of spiral spin correlations. To investigate this model, a non-linear sigma model is used in which disorder is introduced via a randomly fluctuating gauge field. A renormalization group study shows that the collinear fixed point of the model is destroyed through the disorder and that the disorder coupling leads to an additive renormalization of the order parameter stiffness. Further, the stability of the spiral state against the formation of topological defects is investigated with the use of the replica trick. A critical disorder strength is found beyond which topological defects proliferate. Comparing our results with experimental data, it is found that for a hole density $x > 0.02$, i.e. in the entire spin glass regime, the disorder strength exceeds the critical threshold. In addition, some experiments are proposed in order to distinguish if the incommensurabilities observed in neutron scattering experiments correspond to a diagonal stripe or a spiral phase.

PACS numbers: 75.10.Nr, 74.72.Dn, 75.50.Ee

I. INTRODUCTION

A. Generalities

This paper discusses the influence of disorder on the properties of weakly hole doped cuprate materials. In cuprates, the superconducting state emerges through chemical doping of a parent compound which is insulating and shows antiferromagnetic (AF) order with a high critical Néel temperature of typically a few hundred Kelvin. As a consequence of chemical doping, the compounds are intrinsically disordered. Especially at weak doping concentrations, disorder is known to strongly influence the behavior of these materials. This is evident in the simplest cuprate superconductor, $\text{La}_{2-x}\text{Sr}_x\text{CuO}_4$, where the superconducting phase emerges via doping directly from a low temperature spin glass (SG) phase. Recently, glassy characteristics were detected even inside the superconducting phase (see Ref.¹ for a summary of the available experimental data).

Understanding the very weak doping regime of cuprates, the insulating AF and SG regime, should be relatively simple. This optimism is based on the belief that this regime is dominated by the behavior of isolated holes in presence of well developed AF moments. The single hole properties seem now to be quite well understood and early theories of high temperature superconductivity were constructed from these one-hole wave functions. Shraiman and Siggia^{2,3} proposed a theory of interacting hole-quasiparticles based on the one-hole picture and predicted the formation of spiral correlations with a pitch proportional to the hole density. Exper-

iments have to date however not found any evidence of such spiral correlations inside the superconducting phase. The pairing mechanism suggested by this semiclassical picture, a dipole-dipole interaction between holes mediated by soft spin waves,^{4,5} has, perhaps unfairly, received scant attention of late. A potential weakness of the approach is the semiclassical treatment of spins (large S), which implies the assumption of a large AF correlation length, whereas in the superconducting phase the spins are believed to form some kind of quantum disordered spin liquid. The scattering of holes by spin excitations would then be qualitatively different at large scales. However, while the semiclassical theory is formulated for large scales, the structure and energy of the resulting two-hole bound state is determined by the shortest cutoff in the system⁵, where AF correlations are still intact. Furthermore, the correlation length can be substantial even in superconducting samples, e.g. it exceeds 200 Å in the stripe compound $\text{La}_{1.45}\text{Nd}_{0.4}\text{Sr}_{0.15}\text{CuO}_4$.⁶ Thus, the pairing mechanism suggested by the semiclassical picture may hide some truth despite the absence of long range order.

While a semiclassical approach to the superconducting regime may or may not be valid, at sufficiently low hole concentrations, where static AF correlations are still dominant, i. e. in the SG and AF phase, a semiclassical treatment of spins is certainly justified. However, at these low densities, where the system is still a Mott insulator, screening is very poor and long-range Coulomb interaction leads to a strong disorder potential which must be taken into account. Here we discuss a model in which the entire charge distribution is assumed to be quenched. Each hole, localized close to an ionized dopant, is as-

sumed to produce a long-ranged dipolar-shaped frustration of the AF, similar to the one known to be produced by delocalized holes. A polarization of the dipole moments then implies the appearance of spiral correlations.

It is known that the spiral state described by Shraiman and Siggia, if one ignores disorder, is unstable toward a local enhancement of the spiral pitch. This instability arises from the fermionic susceptibility of the holes and may signal an instability towards charge density formation or phase separation.⁷ However, if the holes are quenched this instability is suppressed. Therefore, disorder takes a prominent role in the creation of a spiral state.

We here develop a renormalization approach for disordered spiral phases, where we study the scaling of the spin stiffness and of the disorder. The importance of topological defects of the spiral texture is analyzed and their relevance for the physics of the spin glass phase is discussed.

B. Undoped and weakly doped cuprates

Undoped La_2CuO_4 is a charge transfer insulator with an antiferromagnetically ordered ground-state. It is well described by a simple square lattice spin-1/2 Heisenberg model,

$$H_H = J \sum_{\langle ij \rangle} \mathbf{S}_i \cdot \mathbf{S}_j, \quad (1)$$

with the antiferromagnetic exchange $J \sim 1200\text{K}$. The sum is over nearest neighbor pairs of sites and \mathbf{S}_i are spin-1/2 operators.

In the study of magnetism of La_2CuO_4 , an approach based on the quantum-non-linear- σ model (QNL σ M) has been highly successful. It correctly describes the long wavelength hydrodynamic modes (spin waves) of the Heisenberg model.⁸ In this continuum model, it is assumed that the antiferromagnetic correlation length is much larger than the lattice spacing and the model describes slow fluctuations of the locally well defined staggered magnetization \mathbf{n} (with $\mathbf{n}^2 = 1$). The QNL σ M action is

$$\frac{S_{\text{eff}}}{\hbar} = \frac{\rho_S}{2\hbar} \int_0^{\hbar\beta} d\tau \int d^2\mathbf{x} \left\{ (\partial_\mu \mathbf{n})^2 + \frac{1}{c^2} (\partial_\tau \mathbf{n})^2 \right\}. \quad (2)$$

The spin stiffness ρ_S and the spin wave velocity c should be viewed as phenomenological parameters to be determined either from experiment or from other techniques such as spin wave theory or numerical simulations. The coupling constant of the model is $g = \hbar c \Lambda / \rho_S$ (Λ is a high frequency cutoff). There is a zero temperature quantum phase transition at $g = g_c \sim 4\pi$ from a phase with long-range order ($g < g_c$, “renormalized classical regime”) to a phase which exists for $g > g_c$ and which is quantum disordered with only finite spin correlations and no static magnetic order. It is now firmly believed that the

$S = 1/2$ Heisenberg model described by (1) has $g < g_c$. Measurements of the correlation length of La_2CuO_4 have been fitted extremely well with the QNL σ M predictions for the renormalized classical regime.⁹

Once holes are added to the CuO_2 planes, the magnetism becomes rather complex. Fig. 1 summarizes the magnetic phase diagram at weak doping concentrations of $\text{La}_{2-x}\text{Sr}_x\text{CuO}_4$ and $\text{Y}_{1-x}\text{Ca}_x\text{Ba}_2\text{CuO}_4$.¹⁰ Here, we concentrate on $\text{La}_{2-x}\text{Sr}_x\text{CuO}_4$. For very small Sr concentration, the most dramatic effect is a rapid reduction of T_N with the complete destruction of long-range order occurring at a critical doping value of roughly $x_g \sim 0.02$. Further, a spin freezing is observed inside the AF phase below a temperature T_f which scales linearly with the Sr concentration, $T_f \sim (815\text{K})x$ for $0 < x < x_g$. This spin freezing is inferred from a broad distribution of extremely slow relaxation times measured with local probes such as ^{139}La nuclear quadrupole resonance¹¹ (NQR) and muon spin resonance¹² (μSR). Surprisingly, while at higher temperatures doping leads to a reduction of the local staggered moments, at temperatures lower than about 30 K the staggered moments recover and at zero temperature they are practically doping independent and approach the value of the undoped compound,^{11,12} see the middle panel of Fig. 1. However, the distribution of staggered moments is broad at finite doping, with a variance which is again simply linear in x , see Fig. 1 bottom.¹⁰ Both the recovery of the staggered moments and the broad distribution of relaxation times are reminiscent of a transverse spin glass state, in which the transverse spin wave modes of the AF freeze in a static but random pattern. These are clear signatures of disorder in the weakly doped AF phase. This is further corroborated by transport measurements, which show a behavior typical for random systems.¹³ At temperatures below ~ 50 K the conductivity roughly follows variable range hopping characteristics while at higher temperatures a thermally activated conductivity is observed, with activation energies of about 19 meV.¹⁴ This indicates that the holes localize near the randomly distributed Sr donors.

Both the presence of finite staggered magnetic moments and the broad distribution of slow relaxation times persist also above $x > x_g$ where long-range order is destroyed.¹⁰ Again, there is a recovery of the staggered moments at very low temperatures, although the zero temperature moment is now slightly smaller than in the undoped compound. The x dependence of T_f follows now roughly a $1/x$ scaling. The regime $0.02 < x < 0.05$ is well described as a conventional spin glass (SG) and shows characteristic non-ergodic behavior.¹⁵ The freezing transition temperature T_f in this regime can thus be identified as a SG transition temperature T_g . The fact that staggered moments persist also above $x = 0.02$ is important and excludes the possibility that the transition at $x = 0.02$ is a disordering transition driven by quantum fluctuations as described in the QNL σ M formulation above. It is often argued that upon hole doping, the reshuffling of the spins by mobile holes leads to en-

hanced quantum fluctuations of the spins which would eventually drive the spin system past the quantum critical point of the QNL σ model, driving the AF into a spin liquid phase. As the transition at $x = 0.02$ is not followed by a spin liquid phase but rather a SG this scenario does not apply for the AF-SG transition.

Only recently, it was found that the short ranged magnetic order in the SG regime is incommensurate, with a maximum of the imaginary part of the susceptibility located at the in-plane wave vector $(1/2 \pm \delta/\sqrt{2}, 1/2 \mp \delta/\sqrt{2})$, in units of $2\pi/a$ where a is the Cu lattice spacing.^{15,16,17} Here, δ is the incommensurability which roughly follows $\delta \simeq x$. This incommensurability has often been interpreted as diagonal stripe formation, even though no signatures of a charge modulation were observed. Rather, all experiments point toward a quenched charge distribution and we thus argue that a more likely explanation is the formation of short ranged spiral order.

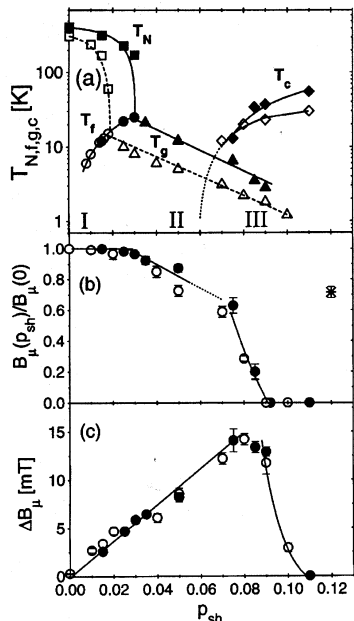


FIG. 1: Phase diagram as seen by μ -SR, with data obtained from $\text{La}_{2-x}\text{Sr}_x\text{CuO}_4$ (open symbols) and $\text{Y}_{1-x}\text{Ca}_x\text{Ba}_2\text{CuO}_3$ (closed symbols), p_{sh} is the hole concentration. (a) Doping dependence of the Néel temperature T_N , freezing transition temperature T_f , spin glass transition temperature T_g and superconducting transition temperature T_c . (b) Normalized average internal field at $T=1$ K. (c) RMS deviation ΔB at $T=1$ K. Fig. from Niedermayer *et al.*¹⁰

In $\text{La}_{2-x}\text{Sr}_x\text{CuO}_4$ static AF moments are strong for small x and the holes seem to localize at low temperatures where transport experiments indicate a relatively weakly bound hole with a localization length of a few lattice constants. Thus, one might hope to gain considerable insight into these phases by solving the one-hole problem first and to proceed from there on. As mentioned in the beginning, the understanding of the spin-polaron state arising from one hole in an antiferromagnetic background

is by now quite mature.^{2,18,19} For the $t - J$ model, the bottom of the dressed hole band lies at the zone face centers $\mathbf{k}_0 = (\pm\pi/2, \pm\pi/2)$ and the bandwidth scales with J . Because of the presence of two sub-lattices, there exists a pseudo-spin degeneracy for each \mathbf{k} vector. An important characteristic of the hole wave function is that it describes a long-ranged dipolar distortion of the AF order which arises from a coupling of the spin current carried by the hole to the magnetization current of the AF background.² Relative to the position of the moving hole, the Fourier transform of the transverse spin deviations is then proportional to $(\bar{\mathbf{q}}_x + \bar{\mathbf{q}}_y)/\bar{q}^2$,¹⁸ where $\bar{\mathbf{q}} = \mathbf{q} - (\pi, \pi)$, i.e. the staggered magnetization shows a dipolar pattern in real space identical to the one produced by an isolated ferromagnetic bond, see Sec. II A.

The Sr impurity position, located above the center of a Cu plaquette, has a high symmetry and couples to both sub-lattices in the same way, so that the pseudo-spin degeneracy mentioned above should survive also in the bound hole state. The bound hole state is a superposition of plane wave states describing the mobile hole. For sufficiently weakly bound holes, we expect the main weight of the bound hole wave function to remain at wave vectors close to \mathbf{k}_0 or equivalent positions, and, depending on the relative phases and the weight of these pockets, dipolar or quadrupolar frustration is associated with the localized hole. We note that dipolar frustration was also suggested by Aharony *et al.* for O doped systems, caused by a localization of holes in the O site with the liberation of one of the spins from the O p^6 state,²¹ leading to an effective ferromagnetic coupling for the two Cu spins joint by the O. While the microscopic origin of frustration in the Aharony model is very different from the quantum mechanical one that we assume here, the phenomenological spin-only model we employ below is not sensitive to the microscopic details. In either case, the dipole moment of the localized hole state is characterized by two vectors, one in spin- and one in real space. The real space vector characterizing the dipole is simply the orientation of the ferromagnetic bond in the Aharony picture while it is determined by the four coefficients $c_{\mathbf{k}_0}$ and by the equivalent wave vectors of the bound hole wave function in the quantum mechanical model. The coupling to the spin background is then identical in both models. Here we simply assume that the localized hole produces dipolar frustration and, rather than relating our phenomenological coupling parameters to a microscopic model, we derive our parameters from a comparison to experiments. As we discuss below, the dipole model can quite well explain all the important characteristics of the magnetism of the weakly doped AF and SG phase. Let us further mention that for Sr doping, it was proposed that a chiral spin current is induced on the four Cu sites closest to the Sr impurity which leads to a Skyrmion-like distortion of the AF, where the mechanism of frustration is again the coupling between spin and background magnetization currents.²⁰

In section II we introduce the dipolar frustration

model, summarize the main results of previous studies on this model, and discuss how they compare with experiments. In section III we first derive an extension of the model to allow for non-collinear correlations which arise from dipole ordering. We perform a RG calculation to understand the influence of disorder and discuss the importance of topological defects of the spin texture. Finally, in section IV our results are compared with neutron scattering data on the SG phase of $\text{La}_{2-x}\text{Sr}_x\text{CuO}_4$. We find that the SG phase can be described as a strongly disordered spiral phase in which topological defects proliferate.

II. THE AF PHASE AND DIPOLAR FRUSTRATION MODELS

We briefly sketch here the basis of the dipolar frustration model and the results of previous studies of this model in the collinear limit. The model as presented in this section is applicable only for the antiferromagnetic phase in which the dipoles do not have a preferred direction. At high temperatures, the collinear theory can then be used. We will show in the next section however, that the collinear model is not able to describe the low temperature and/or strong disorder regime, where non-collinear behavior emerges.

In the dipole model, it is assumed that each localized hole produces dipolar frustration. It is then possible to study the magnetism of the hole doped materials completely ignoring the charge degrees of freedom and to work with the spin sector only. Further, as there are clear indications of static AF correlations for $x < 0.05$, the antiferromagnet should be well described within the renormalized classical regime of the QNL σ M. In this regime, quantum fluctuations simply lead to a renormalization of the coupling constant of the classical model. A classical model should thus suffice to describe the relevant physics in the AF and SG regime.

A. Ferromagnetic bonds as an example of dipolar frustration

Dipolar frustration was first discussed in the general context of insulating spin glasses by Villain.²² The simplest way of producing dipolar spin textures is by placing a ferromagnetic bond in an otherwise AF magnet, whose order parameter we denote by \mathbf{n} . At a distance \mathbf{x} away from the ferromagnetic bond, this leads to a deviation of the Néel order $\delta\mathbf{n} \sim \mathbf{f}_\mu x_\mu/x^2$. Here, \mathbf{f}_μ is a vector both in spin and lattice space, where $\mu = 1, 2$ are the indices of the 2D lattice vector. The spin part corresponds to the local ferromagnetic moment (with $\mathbf{f}_\mu \perp \mathbf{n}$) produced by the bond and the lattice part corresponds to the orientation of the bond on the lattice (see Fig. 2). This can be easily derived in a harmonic continuum approximation, where the energy density of the magnet away from

the impurity is proportional to $[\partial_\mu(\delta\mathbf{n})]^2$ and the classical equation of motion is $\nabla^2(\delta\mathbf{n}) = 0$. For any impurity distribution, the solution for $\delta\mathbf{n}$ can thus be written in a multipole expansion. As the monopole moment is energetically too costly²² the lowest order contributions, consistent with the symmetry of the one-bond problem, are dipolar.

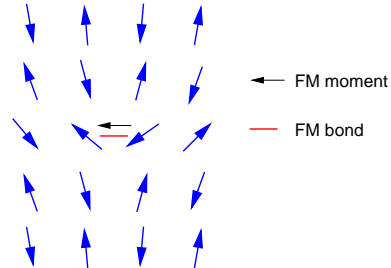


FIG. 2: Dipolar distortions produced by a ferromagnetic bond

B. Collinear Model

Because of the long-range nature of dipolar frustration, a continuum field theory, such as a (classical) non-linear σ -model (NL σ M), should be well suited for a treatment of this problem. While the dipole spin structure discussed above is a solution of the harmonic theory, it is not a solution of the 2D NL σ M. Nonetheless one can study the dipole model within the NL σ M, if one introduces the dipolar frustration through a minimal coupling scheme. As mentioned in Ref. [23], the dipolar frustration can be reproduced (on the harmonic level) via a coupling of the dipoles to the gradient of the order parameter \mathbf{n} of the NL σ M. Thus, within a NL σ M approach, the reduced Hamiltonian of the model can be written as^{23,24} (the factor $\beta = T^{-1}$ is included in the Hamiltonian and we set $k_B=1$)

$$H_{\text{col}} = \frac{\rho_s}{2T} \int d^2\mathbf{x} (\partial_\mu \mathbf{n})^2 + \frac{\rho_s}{T} \int d^2\mathbf{x} \mathbf{f}_\mu \cdot \partial_\mu \mathbf{n} \quad (3)$$

where $\mathbf{n}^2 = 1$, ρ_s is the spin stiffness (renormalized by quantum fluctuations), T the temperature, \mathbf{n} a three component unit vector representing the local staggered moment and \mathbf{f}_μ is a field representing the dipoles. We did not include here small corrections which lower the spin symmetry from Heisenberg to XY or Ising. While these are known to be present both in the undoped and weakly doped compounds²⁵, they have a very small characteristic energy scale and, as a first approximation, we set them to zero. Note however that these terms dominate the static magnetic susceptibility near the Néel transition. For a random distribution of localized dipoles we write

$$\mathbf{f}_\mu(\mathbf{x}) = \mathcal{M} \sum_i \delta(\mathbf{x} - \mathbf{x}_i) a_\mu(\mathbf{x}_i) \mathbf{M}_i \quad (4)$$

where the sum is over the impurity sites, \mathbf{a}_i are lattice unit vectors, \mathbf{M}_i unit vectors in spin space, and \mathcal{M} measures the strength of the dipoles. While there is no dipole-dipole interaction term in Eq. (3), fluctuations of the \mathbf{n} field generate a spin wave mediated interaction. This can be seen once short scale fluctuations are integrated out under a renormalization procedure.²³ An integration over the short scale fluctuations up to a scale $L \gg 1/\sqrt{x}$ (but $L \ll \xi$ where ξ is the 2D spin correlation length) leads to an effective interaction term of the form

$$H[\{\mathbf{M}_i\}] = \frac{\rho_s \mathcal{M}^2}{2T} \sum_{i,j} J_{ij} \mathbf{M}_i \cdot \mathbf{M}_j \quad (5)$$

with

$$J_{ij} = \frac{1}{2\pi x_{ij}^2} \left(2 \frac{(\mathbf{x}_{ij} \cdot \mathbf{a}_i)(\mathbf{x}_{ij} \cdot \mathbf{a}_j)}{x_{ij}^2} - \mathbf{a}_i \cdot \mathbf{a}_j \right), \quad (6)$$

and $\mathbf{x}_{ij} = \mathbf{x}_i - \mathbf{x}_j$. Thus, for an average separation of dipoles $\sim 1/\sqrt{x}$ there is a random interaction among dipoles with a characteristic energy $U \sim \rho_s \mathcal{M}^2 x / 4\pi$. It was further shown²³ that at high temperatures, $U \ll T$, the presence of dipoles lead to a renormalized effective stiffness $\rho_{\text{eff}} = \rho_s(1 - U/T)$. Thus, the correlation length at high temperatures (and small x) has the form

$$\xi \sim \exp\left(\frac{2\pi\rho_{\text{eff}}}{T}\right) = \exp\left(\frac{2\pi\rho_s}{T} - \frac{2\pi\rho_s U}{T^2}\right). \quad (7)$$

This result agrees to lowest order in x with that obtained by Cherepanov *et al.*²⁴ in a related renormalization group (RG) calculation where they calculated ρ_{eff} up to order x^2 . From a comparison with correlation lengths obtained from neutron scattering data at high temperatures, they estimated $U \sim 20\rho_s x$. The doping dependence of T_N was also found to be consistent with the dipole model.²⁴

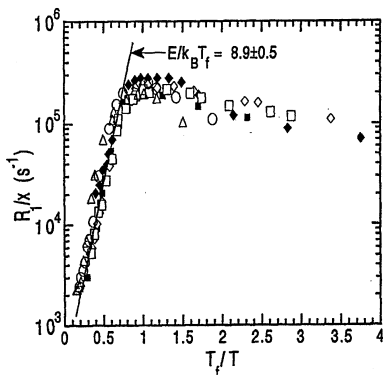


FIG. 3: $R_1 = (T_1^*)^{-1}$ data from ^{139}La NQR relaxation measurements for $\text{La}_{2-x}\text{Sr}_x\text{CuO}_4$ and various $x < 0.02$, from Ref. [11].

A second independent test of the value of U is to consider the spin relaxation times inside the AF phase.

This can be understood already within the theoretical framework just presented, using arguments similar to those from Ref.²⁶ where spin relaxation has been discussed within a slightly different frustration model. The relaxation rates inside the AF phase can be explained within the dipole theory if one assumes that the relaxation is driven by the interaction among dipoles and hence controlled by the parameter U . At temperatures well above the actual freezing temperature, an Arrhenius law is observed, with a characteristic energy $E = 8.9T_f \sim 7250Kx$, see Fig. 3. The above estimate of U correctly reproduces the linear scaling of the relaxation energy with x and also gives a good estimate for the slope. With $U = 20\rho_s x$, $\rho_s \sim 24 \text{ meV}$ ²⁴ one obtains $U \sim 5500Kx$. Considering that this is a very rough approximation, the value is not too far off from the experimental one. We mention further that the linear scaling of the width of the distribution of local staggered moments is also consistent with a dipole model.²⁷

III. NON-COLLINEAR CORRELATIONS AND DIPOLE ORDERING

While the dipole model presented above can well explain the temperature and doping dependence of the correlation length not just in the AF but also, to some extent, in the SG regime,²⁴ theoretical investigations of the model have always predicted (or rather assumed) short ranged commensurate antiferromagnetism. The recent observation of incommensurate (IC) correlations for the regime $0.02 < x < 0.05$ requires therefore a new approach to the SG phase.²⁸

As a possible explanation for the presence of IC correlations, a disordered striped phase has been proposed, similar to the ordered striped phase found near $x \sim 1/8$. While there is indeed an instability in the striped phase toward a disordered phase at low x ,²⁹ it is unlikely that the stripes will survive in presence of strong disorder. In fact, recent numerical simulations of Shraimann-Siggia dipoles with disorder have shown that the latter leads to a destruction of the stripe phase.³⁰

In the spin glass regime, there are two competing length scales. The first is related to the average separation between disorder centers (Sr ions) l_d which scales as $l_d \sim 1/\sqrt{x}$. The other is the scaling of the periodicity l_s associated with the incommensurability, which scales as $l_s \sim 1/x$. For small x , $l_d \ll l_s$. In a stripe scenario the charge distribution would also have a periodicity which scales with l_s . Thus, in a striped phase the charge can not take full advantage of the disorder. The stripes must either break up into short segments or reduce their on-stripe charge density considerably to take advantage of the disorder potential. Instead we propose here a theory in which the charges are completely disordered and the incommensurability exists only in the spin sector. Then, there is no conflict between the two scales l_s and l_d as l_s relates only to the spins whereas l_d characterizes the

charge distribution.

Notice that even in the case that short segments of stripes should be present, these stripes would lose their anti-phase domain wall character and instead act like a row of ferromagnetic bonds, again causing dipolar frustration. Thus, the theory we present here applies both to the case of localized hole states which produce dipolar frustration as it does to a system of randomly placed stripe segments. We view the scenario of localized holes however as the more plausible one.

A. Dipole ordering

It is easy to see how the dipole model can lead to IC correlations.³ The Hamiltonian Eq. (3) favors the formation of a spiral phase, with a non-zero average twist $\partial_\mu \mathbf{n}$ of the AF order and a simultaneous alignment of the dipoles, $\langle \mathbf{f}_\mu \rangle \neq 0$, as long as the lattice and spin degrees of freedom of dipoles are annealed and free to orient themselves. The lattice position of the Sr dopants (located above the center of a Cu plaquette), which pin the holes, suggests that this freedom indeed exists. We emphasize that a spatially homogeneous distribution of dipoles is not required for the formation of spiral correlations.

The preferred orientation of the lattice part of the \mathbf{f}_μ vector is determined by the nature of the localized hole state and therefore should reflect the symmetries of the underlying lattice. Thus a discrete set of favored lattice vectors for the formation of the spiral exists. The a - b (or square lattice) symmetry breaking associated with the formation of spiral correlations can therefore have truly long range order. The continuous symmetry of spin space on the other hand inhibits long-range magnetic order in the 2D system for either finite temperatures or disorder. The experimental observation of a macroscopic a - b asymmetry¹⁶ but very short spin correlation lengths thus clearly motivate the study of the dipole model.

B. Continuum description of spiral phases

We here investigate the dipole model allowing for the presence of non-zero ordered moments but assume a random spatial distribution of the dipoles. First, however, we need a proper theoretical description of the homogeneous spiral phase.

In collinear magnets, the rotational $O(3)$ symmetry of the system is broken down to a ground state with $O(2)$ symmetry, as rotations around the magnetization axis leave the ground state invariant (this is schematically shown on the left hand side of Fig. 4). The order parameter of collinear magnets is then an element of $O(3)/O(2)$. This group is isomorphic to the group of three dimensional unit vectors \mathbf{n} , which is the representation used in the Hamiltonian Eq. (3). Further, in absence of dipoles, the Hamiltonian Eq. (3) is invariant with respect to $O(2)$ rotations of the lattice variables.

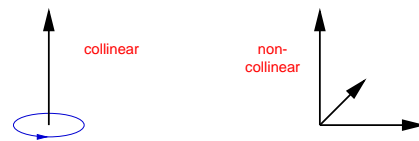


FIG. 4: The order parameter of collinear magnets, which are invariant under rotations around the collinear axis, can be represented by a unit vector (left), whereas non-collinear order parameters require three orthonormal vectors (right).

The spin and lattice symmetries are decoupled and independent for the collinear AF. A spiral ground state on the other hand breaks the $O(3)$ spin symmetry completely. Moreover, in a spiral state the lattice symmetries and the spin symmetries are no longer decoupled and the order parameter space of such a state becomes more involved.

For spirals, the combined symmetry of lattice and the spin space is $O(3) \times O(2)$. As discussed in detail by Azaria *et al.*,³¹ the coupling of the spin and lattice degrees of freedom in frustrated spin systems leads to an order parameter which results from a symmetry breaking of the combined lattice and spin degrees of freedom and is in general of the form $O(3) \times O(q)/O(q)$ where q depends on the symmetries of the lattice. For a spiral phase, one finds³² $q = 2$.

A convenient representation of the order parameter is in terms of orthonormal \mathbf{n}_k , $k = 1 \dots 3$, with $n_k^a n_q^a = \delta_{kq}$. Klee and Muramatsu³² have derived a continuum field theory for the \mathbf{n}_k order parameters from the lattice Heisenberg model Eq. (1), assuming an IC spiral state with an ordering wave vector $\mathbf{k}_S = (\frac{\pi}{a}, \frac{\pi}{a}) + \mathbf{q}_S$. Here, \mathbf{q}_S measures the deviation from the commensurate AF wave vector, see Fig. 5. The lattice spins \mathbf{S}_i at sites \mathbf{r}_i can be parametrized in a spiral configuration with the use of the n_k^a as (with $\mathbf{n}_3 = \mathbf{n}_1 \times \mathbf{n}_2$)

$$\mathbf{S}_i/S = \mathbf{n}_1 \cos(\mathbf{k}_S \cdot \mathbf{r}_i) - \mathbf{n}_2 \sin(\mathbf{k}_S \cdot \mathbf{r}_i). \quad (8)$$

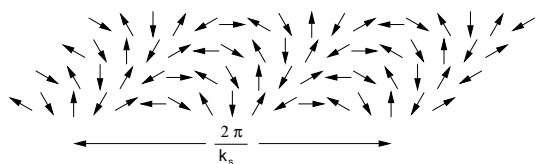


FIG. 5: Spin texture of an AF spiral.

A perfectly ordered spiral is described by Eq. (8) with constant, i.e. space independent, \mathbf{n}_k . To allow for spatial fluctuations of the spins around the spiral order, Klee and Muramatsu introduced a slowly varying field \mathbf{L} via^{32,33}

$$\begin{aligned} \frac{\mathbf{S}(\mathbf{r}_i)}{S} &= \frac{\mathbf{N} + a\mathbf{L}}{\sqrt{1 + 2a\mathbf{N} \cdot \mathbf{L} + a^2 L^2}} \\ &= \mathbf{N} + a [\mathbf{L} - (\mathbf{N} \cdot \mathbf{L})] - a^2 \left[(\mathbf{N} \cdot \mathbf{L}) \mathbf{L} + \frac{1}{2} L^2 \mathbf{N} \right] \end{aligned}$$

$$- \frac{3}{2} (\mathbf{N} \cdot \mathbf{L})^2 \mathbf{N} \Big] + \mathcal{O}(a^3), \quad (9)$$

where $\mathbf{N} = \mathbf{n}_1 \cos(\mathbf{k}_S \cdot \mathbf{r}_i) - \mathbf{n}_2 \sin(\mathbf{k}_S \cdot \mathbf{r}_i)$ with now slowly fluctuating fields \mathbf{n}_k . The continuum theory can then be found upon expressing in the lattice Heisenberg model the spin operators in terms of the \mathbf{n}_k and \mathbf{L} fields, expanding the terms up to order a^2 and taking the limit $a \rightarrow 0$ in the end. After integrating out the \mathbf{L} fields, one finds an effective Hamiltonian which can be written in the classical limit in the general form³² (again we include the factor $\beta = T^{-1}$ into H)

$$H = \frac{1}{2} \int d^2\mathbf{x} p_{k\mu} (\partial_\mu \mathbf{n}_k)^2 + s_\mu \int d^2\mathbf{x} \mathbf{n}_1 \cdot \partial_\mu \mathbf{n}_2. \quad (10)$$

This description is valid for length scales larger than $|\mathbf{q}_S|^{-1}$. The stiffnesses of the order parameter \mathbf{n}_k are given initially by $p_{1\mu} = p_{2\mu} = JS^2 \cos(q_S \mu a)/(2T)$ and $p_{3\mu} \simeq 0$, but will change under a renormalization of the model. We will ignore for the most part the small anisotropy (of order $q_S^2 a^2$) in the stiffnesses $p_{k\mu}$ and just write p_k . The vector \mathbf{s} is to lowest order given by $\mathbf{s} = J\mathbf{q}_S/T$. The term with the s_μ pre-factor makes this Hamiltonian unstable, which simply expresses the fact that the pure Heisenberg model does not support a spiral phase ground state. The s_μ term will however be canceled by a similar term originating from the coupling of the spins to the ordered fraction of the dipoles, relating the incommensurability self-consistently to the ordered moment of the dipoles. In other words, the ordered dipoles stabilize the spiral phase, as expected.

It must be stressed that because the continuum model is only valid at length scales larger than the period of the IC structure, there is a relatively large uncertainty in the estimates of the $p_{k\mu}$. There is always a fundamental problem in relating the continuum model parameters to those of the original microscopic lattice model, but in this case this problem is especially severe. The continuum model parameters must be obtained from an average over one period of the spiral which, for small incommensurabilities, can be rather large. Thus, the above estimates for the $p_{k\mu}$'s should be taken with care.

C. Disorder coupling: a gauge glass model

We now must include the coupling of the dipolar frustration centers to the spiral order parameter. While there is no microscopic derivation of this coupling at hand, the fact that the coupling in the collinear model can be expressed within a minimum coupling scheme allows for a simple generalization of the model to non-collinear spin states. We first observe that the ordering wave vector of the spiral, \mathbf{q}_S , is entirely determined by the average orientation of the dipoles. Similarly, local variations of the density or orientation of the dipoles should also modify the local ordering wave vector. Further, to reproduce the strong canting produced by the dipoles, the

coupling should be of first order in the spatial derivative of the spiral order parameter. To generate the frustration produced by the dipoles we thus introduce a minimal coupling³⁴ in the first term of Eq. (10), i.e. we replace $(\partial_\mu \mathbf{n}_k)^2$ with $[(\partial_\mu - i\mathbf{B}_\mu \cdot \mathbf{L})\mathbf{n}_k]^2$ where \mathbf{B}_μ is a random gauge field, representing the dipoles. The components of \mathbf{L} are 3×3 matrix representations of angular momenta which generate rotations about the three spin axes, with

$$-i\mathbf{B}_\mu \cdot \mathbf{L} \mathbf{n}_k = \mathbf{B}_\mu \times \mathbf{n}_k. \quad (11)$$

This coupling has the advantage of relative simplicity combined with a clear physical interpretation: the dipolar fields define the locally preferred wave vector of the spiral, and fluctuations of the dipole fields lead to fluctuations of the wave vector. Further, it reproduces the correct form of the dipole coupling in the collinear limit, as shown below. Let us write $\mathbf{B}_\mu = [\mathbf{B}_\mu]_D + \mathbf{Q}_\mu$ so that $[\mathbf{Q}_\mu]_D = 0$, where $[\dots]_D$ is the disorder average. We then obtain the following Hamiltonian for the spiral in presence of disorder,

$$H = \frac{1}{2} \int d^2\mathbf{x} p_{k\mu} (\partial_\mu \mathbf{n}_k)^2 + \int d^2\mathbf{x} p_k \partial_\mu \mathbf{n}_k \cdot \mathbf{Q}_\mu \times \mathbf{n}_k, \quad (12)$$

where the ordered part of the dipole field cancels the second term in Eq. (10). Thus,

$$p_{k\mu} \partial_\mu \mathbf{n}_k \cdot [\mathbf{B}_\mu]_D \times \mathbf{n}_k + s_\mu \mathbf{n}_1 \cdot \partial_\mu \mathbf{n}_2 = 0. \quad (13)$$

As $\mathbf{q}_S \propto \mathbf{s}$, this equation relates the incommensurability linearly to the density of ordered dipoles. The remaining part of the dipole field, \mathbf{Q}_μ , is a quenched variable with zero mean and we assume Gaussian short ranged statistics,

$$[Q_\mu^a(\mathbf{x}) Q_\nu^b(\mathbf{y})]_D = \lambda \delta(\mathbf{x} - \mathbf{y}) \delta_{ab} \delta_{\mu\nu}. \quad (14)$$

In absence of disorder, the Hamiltonian defined by Eq. (12) has the desired $O(3) \times O(2)/O(2)$ symmetry. The $O(3)$ symmetry is associated with the spin indices a of the n_k^a , while the $O(2)$ symmetry is associated with the lattice indices k and arises because $p_{1\mu} = p_{2\mu}$. Hence, the equality $p_{1\mu} = p_{2\mu}$ is directly related and enforced by the symmetries of the spiral. Note that if all $p_{k\mu}$ are identical, the lattice symmetry is enhanced to $O(3)$. We further see now, that the model reduces to the collinear model Eq. (3) in the case $p_{1,2} = 0$ with $p_3 = \rho_s/T$, $\mathbf{n}_3 = \mathbf{n}$ and $\mathbf{f}_\mu = \mathbf{Q}_\mu \times \mathbf{n}$. Unfortunately it is not possible to reach the collinear limit by sending $\mathbf{q}_S \rightarrow 0$. The reason is that the parameters $p_{k\mu}$ are, within the approximation used in their derivation, independent of the size of the unit cell of the spiral, i.e. in the limit $\mathbf{q}_S \rightarrow 0$, the unit cell size diverges while the parameters $p_{k\mu}$ remain unaffected.

The model defined by Eq. (12) is in fact far more general than its derivation might suggest. In absence of disorder it is applicable to other types of frustrated spin systems with a non-collinear ground-state, such as e. g. the Heisenberg model on a triangular lattice.^{31,33,35} It is conceivable, that certain types of randomness in such

lattices may be well described by the disorder coupling employed here. More importantly, the model Eq. (12) can be viewed as a general model to investigate diluted spin glasses, in which a spin system is frustrated by a small number of impurities. There have been investigations of similar models of spin glasses in the past, most notably by Hertz,³⁴ which however did not account for non-collinear correlations which are known to be essential in spin glasses.³⁶ Our approach has the appeal that it can interpolate between collinear and non-collinear states and thus offers the possibility to study the transition from an ordered collinear magnet to a disordered non-collinear one continuously.

D. Renormalization

We now investigate the renormalization of the model under a change of scale, with the objective to understand the influence of the dipoles on the correlation length of the model. For carrying out the RG calculation, it is of advantage to use a $SU(2)$ representation of the model³⁵ (see also App. A). We therefore write

$$n_k^a = \frac{1}{2} \text{tr} [\sigma^a g \sigma^k g^{-1}] \quad (15)$$

where σ^a are Pauli matrices and $g \in SU(2)$. We further introduce the fields³⁷

$$A_\mu^a = \frac{1}{2i} \text{tr} [\sigma^a g^{-1} \partial_\mu g], \quad (16)$$

which are related to the first spatial derivatives of \mathbf{n}_k through $\partial_\mu n_k^a = 2\epsilon_{ijk} A_\mu^i n_j^a$. Eq. (12) then acquires the form,

$$H = \frac{1}{t_\mu} \int d^2 \mathbf{x} \left[\mathbf{A}_\mu^2 + b A_\mu^{z^2} \right] + 2 \int d^2 \mathbf{x} p_{k\mu} \epsilon_{ijk} \epsilon_{abc} A_\mu^i n_j^a n_k^c Q_\mu^b. \quad (17)$$

where $t_\mu^{-1} = 2(p_{1\mu} + p_{3\mu})$ and $b = (p_{1\mu} - p_{3\mu}) / (p_{1\mu} + p_{3\mu})$. At the point $b = 0$ the symmetry is enhanced to $O(3) \times O(3) / O(3) \simeq O(4) / O(3)$ while at $b = -1$ the model is collinear. For spirals, we have initially $b = 1$.

We first discuss the dimensional scaling behavior of the model (12, 17). We assign the dimension -1 to each spatial dimension so ∂_μ has dimension 1. It follows that the \mathbf{A}_μ fields have a scaling dimension of 1. The scaling dimension of the first term in Eqs. (12, 17) is then $2 - d$ where here $d = 2$. Thus, this term is marginal and an RG analysis is required to study the scaling of the t_μ , b parameters. Local terms containing more than two \mathbf{A}_μ terms have positive dimensions and are irrelevant. Hence, such terms, while they are generated in the perturbative expansion we discuss below, need not be considered.

As was pointed out in Ref. [24], for the disorder choice (14) the model defined by Eq. (3) has a lower critical dimension of two and is thus renormalizable in two dimensions, as can be shown with a general Imry-Ma type argument. The same argument can be used for the present

model. The disorder coupling in Eq. (12) can be rewritten in momentum space as a random field coupling of the form

$$\int \frac{d^2 \mathbf{q}}{(2\pi)^2} \mathbf{n}_k(-\mathbf{q}) \cdot \mathbf{h}_k(\mathbf{q});$$

$$\mathbf{h}_k(\mathbf{q}) = ip_{k\mu} q_\mu \int d^2 \mathbf{x} (\mathbf{Q}_\mu \times \mathbf{n}_k) e^{i\mathbf{q} \cdot \mathbf{x}}$$

where the random fields $\mathbf{h}_k(\mathbf{q})$ have disorder correlations with a momentum dependence $\left[h_k^a(\mathbf{q}) h_{k'}^a(\mathbf{q}') \right]_D \propto \delta(\mathbf{q} - \mathbf{q}') |\mathbf{q}|^\Theta$ with $\Theta = 2$. According to general arguments by Imry and Ma,³⁸ in models with continuous symmetries random fields will destroy long-range order as long as $d < 4 - \Theta$. This implies that in our case $d = 2$ is the lower critical dimension²⁴ and a renormalization group analysis of both the stiffness and the disorder coupling is required.

We now derive the one-loop RG equations. For this, we split the original $SU(2)$ field g into slow and fast modes, $g = \tilde{g} \exp(i \varphi^a \sigma^a)$ and trace out the fast modes φ^a which have fluctuations in the range $[\Lambda^{-1}, 1]$, where we set the original UV cutoff equal to 1. For the one-loop calculation, we need an expansion of Eq. (17) up to second order in φ^a (higher order terms will only contribute at higher loop order of the RG). For the fields \mathbf{n}_k and \mathbf{A}_μ the expansion reads (see App. B for more details)

$$A_\mu^i = \tilde{A}_\mu^i + \partial_\mu \varphi^i + \epsilon_{ijk} \varphi^j \partial_\mu \varphi^k + 2\epsilon_{ijk} \varphi^j \tilde{A}_\mu^k - 2\tilde{A}_\mu^i \varphi^2 + 2\tilde{\mathbf{A}}_\mu \cdot \boldsymbol{\varphi} \varphi^i + \mathcal{O}(\varphi^3),$$

$$n_i^a = \tilde{n}_i^a + 2\epsilon_{ijk} \varphi^j \tilde{n}_k^a + \varphi^j \varphi^k R_{jk}^{ai} + \mathcal{O}(\varphi^3),$$

where

$$R_{jk}^{ai} = \frac{1}{2} \text{tr} \left\{ \sigma^a \tilde{g} \left(\sigma^j \sigma^i \sigma^k - \frac{1}{2} \sigma^j \sigma^k \sigma^i - \frac{1}{2} \sigma^i \sigma^j \sigma^k \right) \tilde{g}^{-1} \right\}.$$

The expansion of the energy functional (17) reads

$$H = \frac{1}{t_\mu} \int d^2 \mathbf{x} \left[\tilde{\mathbf{A}}_\mu^2 + b \left(\tilde{A}_\mu^z \right)^2 \right] + H_{c0} + H_\varphi + H_p \quad (18)$$

with

$$H_{c0} = 2 \int d^2 \mathbf{x} p_{k\mu} \epsilon_{ijk} \epsilon_{abc} \tilde{A}_\mu^i \tilde{n}_j^a \tilde{n}_k^c Q_\mu^b,$$

$$H_p = H_1 + H_2 + H_3 + H_4 + H_{c1} + H_{c2} + H_{c3} + H_{c4}.$$

The first two terms in the expansion of H have exactly the same form as the original functional (17), but are now functionals of the slow fields. H_φ is quadratic in φ and has the form

$$H_\varphi = \frac{1}{t_\mu} \int d^2 \mathbf{x} \left[(\partial_\mu \boldsymbol{\varphi})^2 + b (\partial_\mu \varphi^z)^2 \right]$$

$H_1 \dots H_4$ are generated by the first term in Eq. (17) and are given by

$$H_1 = 2t_\mu^{-1} \int d^2 \mathbf{x} \tilde{A}_\mu^i \partial_\mu \varphi^j \varphi^k \epsilon_{ijk} (1 - b\delta_{iz} + 2b\delta_{jz}),$$

$$\begin{aligned}
H_2 &= 2t_\mu^{-1} \int d^2\mathbf{x} \partial_\mu \varphi^i \tilde{A}_\mu^i (1 + b\delta_{iz}), \\
H_3 &= 4bt_\mu^{-1} \int d^2\mathbf{x} \epsilon_{zjk} \tilde{A}_\mu^z \varphi^j \tilde{A}_\mu^k, \\
H_4 &= 4bt_\mu^{-1} \int d^2\mathbf{x} \left[\left(\epsilon_{zjk} \varphi^j \tilde{A}_\mu^k \right)^2 - \left(\tilde{A}_\mu^z \right)^2 \varphi^2 \right. \\
&\quad \left. + \tilde{A}_\mu^z \varphi^z \tilde{\mathbf{A}}_\mu \cdot \boldsymbol{\varphi} \right].
\end{aligned}$$

The coupling term in Eq. (17) produces the $H_{c1} \dots H_{c4}$ terms,

$$\begin{aligned}
H_{c1} &= 4 \int d^2\mathbf{x} p_{k\mu} \epsilon_{ijk} \epsilon_{abc} \left[\epsilon_{klm} \tilde{n}_j^a \tilde{n}_m^c \tilde{A}_\mu^i \right. \\
&\quad \left. + \epsilon_{jlm} \tilde{n}_k^c \tilde{n}_m^a \tilde{A}_\mu^i + \epsilon_{ilm} \tilde{n}_j^a \tilde{n}_k^c \tilde{A}_\mu^m \right] \varphi^l Q_\mu^b, \\
H_{c2} &= 2 \int d^2\mathbf{x} p_{k\mu} \epsilon_{ijk} \epsilon_{abc} \partial_\mu \varphi^i \tilde{n}_j^a \tilde{n}_k^c Q_\mu^b, \\
H_{c3} &= 2 \int d^2\mathbf{x} p_{k\mu} \epsilon_{ijk} \epsilon_{abc} \left[\tilde{A}_\mu^i \left(\tilde{n}_j^a R_{lm}^{ck} + \tilde{n}_k^c R_{lm}^{aj} \right) \varphi^l \varphi^m \right. \\
&\quad \left. + 2\tilde{n}_j^a \tilde{n}_k^c \left(\tilde{\mathbf{A}}_\mu \cdot \boldsymbol{\varphi} \varphi^i - \tilde{A}_\mu^i \varphi^2 \right) \right. \\
&\quad \left. + 4 \left(\tilde{A}_\mu^i \epsilon_{jlm} \epsilon_{kpq} \tilde{n}_m^a \tilde{n}_q^c + \tilde{A}_\mu^m \epsilon_{ilm} \epsilon_{kpq} \tilde{n}_q^c \tilde{n}_j^a \right) \right. \\
&\quad \left. + \tilde{A}_\mu^m \epsilon_{ilm} \epsilon_{j pq} \tilde{n}_q^a \tilde{n}_k^c \right) \varphi^p \varphi^l \right] Q_\mu^b, \\
H_{c4} &= 2 \int d^2\mathbf{x} p_{k\mu} \epsilon_{ijk} \epsilon_{abc} \left[2 \left(\epsilon_{klm} \tilde{n}_j^a \tilde{n}_m^c \right) \right. \\
&\quad \left. + \epsilon_{jlm} \tilde{n}_m^a \tilde{n}_k^c \right) \partial_\mu \varphi^i \varphi^l + \epsilon_{ilm} \partial_\mu \varphi^m \varphi^l \tilde{n}_j^a \tilde{n}_k^c \right] Q_\mu^b.
\end{aligned}$$

The integration over the fast φ fields is performed with

$$\int \mathcal{D}[\varphi^i] \exp(-H_\varphi) \exp(-H_p) = e^{-\mathcal{F}} \int \mathcal{D}[\varphi^i] \exp(-H_\varphi)$$

where \mathcal{F} is obtained from a cumulant expansion

$$\begin{aligned}
-\mathcal{F} &= \ln \frac{\int \mathcal{D}[\varphi^i] \exp(-H_\varphi) \exp(-H_p)}{\int \mathcal{D}[\varphi^i] \exp(-H_\varphi)} \\
&= \sum_{n=1}^{\infty} \frac{(-1)^n}{n!} \langle H_p^n \rangle_{\varphi c}
\end{aligned} \tag{19}$$

and $\langle \dots \rangle_{\varphi c}$ indicates that only connected diagrams are to be considered.

1. Renormalization of the spin stiffness

We ignore the (small) anisotropy of the t_μ parameter and simply use the isotropic mean $t_s = \sqrt{t_1 t_2}$ in the RG analysis below. We collect all terms in the perturbative expansion which are bilinear in \tilde{A}_μ^i . After performing the disorder average of \mathcal{F} , the renormalized stiffnesses of the \tilde{A}_μ^i fields is found to be (see App. C and D 1)

$$\begin{aligned}
\frac{1}{\tilde{t}_s} &= \frac{1}{t_s} - \left[\frac{2(1-b)}{t_s} + \frac{(2-b+b^2)\lambda}{t_s^2} \right] C^x(\mathbf{0}), \\
\frac{\tilde{b}}{t_s} &= \frac{b}{t_s} - \left[\frac{2b(3+b)}{t_s} + \frac{b(5+b)\lambda}{t_s^2} \right] C^x(\mathbf{0}).
\end{aligned}$$

With $\ell = \ln \Lambda$ and

$$C^x(\mathbf{0}) = \frac{t_s}{4\pi} \ln \Lambda$$

one then finds the RG equations

$$\begin{aligned}
\frac{\partial}{\partial \ell} \frac{1}{t_s} &= -\frac{1-b}{2\pi} - \frac{(2-b+b^2)\lambda}{4\pi t_s}, \\
\frac{\partial}{\partial \ell} \frac{b}{t_s} &= -\frac{(3+b)b}{2\pi} - \frac{(5+b)b\lambda}{4\pi t_s}.
\end{aligned}$$

This yields

$$\frac{\partial}{\partial \ell} t_s = \frac{1-b}{2\pi} t_s^2 + \frac{2-b+b^2}{4\pi} \lambda t_s, \tag{20}$$

$$\frac{\partial}{\partial \ell} b = -\frac{b(1+b)}{\pi} t_s - \frac{b(1+b)(3-b)}{4\pi} \lambda. \tag{21}$$

For $\lambda = 0$, these equations describe the RG of a clean spiral,³⁵ while for the collinear point $b = -1$, the equations reproduce the RG of the stiffness for disordered collinear models.²⁴ From Eq. (21) it is seen that there are two fixed points for b (the asymptotic freedom of the model prevents a true fixed point in 2D as t_s always diverges). The collinear point $b = -1$ is unstable whereas $b = 0$ is stable, irrespective of the disorder. The RG flow of t_s and b is shown in Fig. 6 for $\lambda = 0$. The flow does not change qualitatively for finite λ as long as $\lambda \ll t_s$. Hence, the coupling to weak disorder does not lead to any new fixed points, although the disorder renormalizes the stiffness.

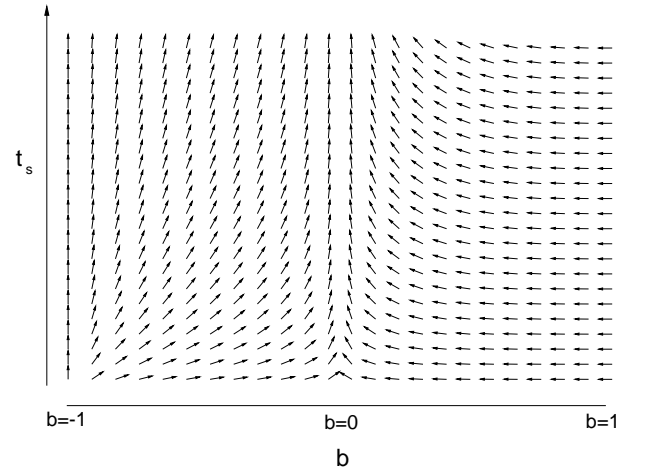


FIG. 6: RG flow of t_s and b for $\lambda = 0$. For any $b > -1$, the flow is toward $b = 0$.

2. Renormalization of disorder coupling

As we discuss below, the renormalization of λ is given by terms proportional to λt_s and λ^2 . As the disorder enters the renormalization of t_s only in the combination

λt_s (see Eq. (20)), we can neglect the renormalization of λ altogether for $t_s \gg \lambda$, i. e. at high temperatures (we have $t_s \propto T/J$). However, for low temperatures the renormalization of λ must be taken into account. To calculate the renormalization of the disorder we follow the approach used in Ref. [24]. In this approach, the renormalized disorder variance is defined by the variance of all terms in the perturbative expansion which couple to the quenched disorder fields and are linear in $\tilde{\mathbf{A}}_\mu$. Note however that there exists no symmetry argument which guarantees that the functional form of the disorder coupling remains unchanged under the RG. It is thus possible that new disorder terms are generated so that a simple renormalization of λ is not sufficient. This is indeed the situation we encounter for general $b \neq 0$ and discuss in more detail below, where we find the generation of new coupling terms at order λ^2 . To find the complete renormalization of the model one would have to include all generated new terms into the original model, which is a rather laborious process which we did not pursue. Nonetheless, as we have just shown above, there are only two possible fixed points even in absence of disorder, $b = 0$ and $b = -1$. Rather than trying to categorize all possible disorder couplings, we therefore focus on a discussion of the RG of the disorder near these two possible fixed points and discuss their stability under the flow.

We begin with the collinear case, $b = -1$. In this case, the renormalized variance of the terms linear in \tilde{A}_μ^i is given by (see App. D 2 and App. D 3, Eq. (D13))

$$\frac{\lambda}{t_s^2} \int d^2\mathbf{x} \left\{ \left[\left(\tilde{A}_\mu^x \right)^2 + \left(\tilde{A}_\mu^y \right)^2 \right] \left(1 - \frac{2}{\pi} t_s \ln \Lambda \right) - \frac{1}{2\pi} \lambda \ln \Lambda \right\} + \left(\tilde{A}_\mu^z \right)^2 \frac{1}{2\pi} \lambda \ln \Lambda \right\}. \quad (22)$$

What is evident from this result is that the renormalized disorder coupling is no longer of the original form $p_k \partial_\mu \mathbf{n}_k \cdot \mathbf{Q}_\mu \times \mathbf{n}_k$. Such a coupling has a variance which includes a prefactor of $(1+b)^2$ of $(\tilde{A}_\mu^z)^2$. According to Eq. (21), $b = -1$ is not changed under the influence of the original disorder coupling. A renormalization which retains the form of the original coupling can then not lead to a renormalized disorder variance with a finite prefactor of $(\tilde{A}_\mu^z)^2$ at $b = -1$. Such a term is however present in Eq. (22) we conclude that a new type of disorder coupling is generated at $b = -1$. This is perhaps easier to see in Fourier space, where the original disorder coupling can be written as a correlated random field coupling $\mathbf{n}_k(-\mathbf{q}) \cdot \mathbf{h}_k(\mathbf{q})$, see Eq. (18). For the original minimal coupling one has $\mathbf{h}_k(\mathbf{q}) \propto p_k$ and thus, in the collinear limit $b = -1$ (or $p_1 = 0$), only \mathbf{n}_3 is affected by this coupling. We can then interpret the finite prefactor of the $(\tilde{A}_\mu^z)^2$ term in the disorder variance as the generation of correlated fields which couple also to $\mathbf{n}_{1,2}$ even at $b = -1$. It is evident that such a coupling will drive the system away from $b = -1$ and thus destroy the collinear fixed point. Thus, even if the original AF order is collinear

(i.e. in absence of dipole ordering), the disorder drives the system to a non-collinear state. An analysis which pre-supposes collinear order is thus not valid in the presence of dipoles and cannot describe the low temperature regime correctly. Physically, one would also expect the appearance of non-collinearity. The random canting of spins leads to a random local deviation of the spins from the ordering axis and thus destroys the remaining $O(2)$ spin symmetry of the collinear model.

To make contact with the RG result obtained from the collinear model in Ref. [24], we note that we can reproduce the result Cherepanov *et al.* obtained for the disorder renormalization if we ignore non-collinear modes. We can then define the renormalization of λ just by the terms which are present in a purely collinear theory, i.e. by the $\left[\left(\tilde{A}_\mu^x \right)^2 + \left(\tilde{A}_\mu^y \right)^2 \right]$ term in Eq. (22). Then

$$\frac{\partial \lambda}{\partial \ell t_s^2} = -\frac{2\lambda}{\pi t_s} - \frac{\lambda^2}{2\pi t_s^2}, \quad (23)$$

which, using Eq. (20) leads to

$$\frac{\partial}{\partial \ell} \lambda = \frac{3}{2\pi} \lambda^2. \quad (24)$$

This, together with Eq. (20) are the RG equations found in Ref. [24] (note that our stiffness t_s differs from the stiffness t used in Ref. [24] by a factor two). We emphasize that this result ignores the role of non-collinearity in the problem.

We now turn to the point $b = 0$, the only remaining possible fixed point of the model. At this highest symmetry point we find that no new coupling terms are generated. The variance of the renormalized disorder coupling takes the form

$$\frac{\lambda}{t_s^2} \int d^2\mathbf{x} \left\{ \tilde{\mathbf{A}}_\mu^2 \left(1 - \frac{4t_s + 3\lambda}{4\pi} \ln \Lambda \right) \right\}. \quad (25)$$

Thus,

$$\frac{\partial \lambda}{\partial \ell t_s^2} = -\frac{1}{\pi} \frac{\lambda}{t_s} - \frac{3}{4\pi} \frac{\lambda^2}{t_s^2} \quad (26)$$

which yields the RG equation, valid for $b = 0$ but any initial ratio of λ/t_s ,

$$\frac{\partial}{\partial \ell} \lambda = \frac{\lambda^2}{4\pi}. \quad (27)$$

Using Eq. (20), we can simplify this through $z = t_s + \lambda/2$ to get

$$\frac{\partial}{\partial \ell} z = \frac{1}{2\pi} z^2. \quad (28)$$

So for $b = 0$ the presence of disorder leads to an additive renormalization of the stiffness, $t_s \rightarrow t_s + \lambda/2$. In presence of any amount of disorder, the IC correlation length ξ at $T = 0$ is finite, as can be inferred from

an integration of the RG equation with $b = 0$, yielding $\xi \propto \exp(C(t_{s0} + \lambda_0/2)^{-1})$ with some cutoff dependent constant C . Thus, even at $T = 0$, $\xi \propto \exp(2C\lambda_0^{-1})$ is finite. While the disorder scales to strong coupling, the relative disorder strength with respect to the stiffness, λ/t_s , always scales to zero so that at long wavelengths the disorder becomes less relevant. This is surprisingly different to the situation with $b = -1$ fixed,²⁴ where the ratio λ/t_s was found to diverge below a certain initial value of λ_0/t_{s0} which was interpreted as the scaling toward a new disorder dominated regime. Thus, if one correctly takes into account the non-collinearity, this disorder dominated phase disappears. The absence of a sharp cross over from a weak disorder to a strong disorder regime is certainly surprising, especially as the experiments clearly observe a transition into a spin glass phase at a finite temperature.¹⁵ The finite temperature transition may be related to the presence of inter-layer coupling. We argue below, however, that topological defects can alter the RG behavior considerably and may be a more natural explanation for the appearance of a strong disorder regime.

E. Topological defects: saddle point treatment

The RG results presented above do not take into account topological defects³⁹ of the spiral as only spin waves excitations enter the calculation. As is well known from XY spin models, topological defects can play an important role and drive finite temperature transitions.⁴⁰ The neglect of topological defects has been a source of criticism toward the NL σ M approach to frustrated magnets, which gives controversial results for $\epsilon = 1, 2$ in an ϵ expansion around $D = 2 + \epsilon$ dimensions.⁴¹ For two dimensional systems, the NL σ M results were however found to be in very good agreement with numerical simulations as long as the temperatures were sufficiently low.⁴² Only at higher temperatures, a deviation from the NL σ M predictions for the temperature dependence of the correlation length was observed which was attributed to the appearance of isolated topological defects. In the numerical simulations the high temperature region showed some resemblance to the high temperature region of XY-models⁴² which indicates that this region is characterized by free defects. However, at present a good understanding of the influence of such defects in non-collinear systems is still lacking.⁴¹

The topological defects of spirals have their origin in the chiral degeneracy of the spiral, i.e. the spiral can turn clock- or anti-clock wise.⁴¹ At a topological defect, the spiral changes its chirality. As the chirality takes only two possible values, the defects are Z_2 defects.

It is then straightforward to find topological defect solutions of the saddle point equations of a clean spiral.³⁹ The saddle point equations can be obtained from the perturbative expansion of the energy density, Eq. (18-19). One finds that extremal solutions must satisfy for each

$j = x, y, z$ the equations

$$(1 + b\delta_{jz}) \partial_\mu A_\mu^j = 2b\epsilon_{zjk} A_\mu^z A_\mu^k, \quad (29)$$

where j is not summed over. For $b > -1$ one finds solutions of the form³⁹

$$g_s(\mathbf{x}) = \exp\left(\frac{i}{2} m^a \sigma^a \Psi(\mathbf{x})\right), \quad (30)$$

where \mathbf{m} is a space independent unit vector and $\Psi(\mathbf{x})$ a scalar function. With this Ansatz, one has $A_\mu^i(\mathbf{x}) = \frac{1}{2} m^i \partial_\mu \Psi(\mathbf{x})$ and thus, upon insertion into Eq. (29), one finds for \mathbf{m} and Ψ the equations (j is again not summed over)

$$(1 + b\delta_{jz}) m^j \partial_\mu^2 \Psi(\mathbf{x}) = b\epsilon_{zjk} m^z m^k (\partial_\mu \Psi(\mathbf{x}))^2. \quad (31)$$

The weight of the configuration described by g_s is given by (we set $t_\mu = t_s$)

$$\begin{aligned} H[g_s] &= \frac{1}{t_s} \int d^2\mathbf{x} \left[\mathbf{A}_\mu^2 + b (A_\mu^z)^2 \right] \\ &= \frac{1}{4t_s} \left[1 + b (m^z)^2 \right] \int d^2\mathbf{x} (\partial_\mu \Psi)^2. \end{aligned} \quad (32)$$

We see that for $b < 0$, the energy is minimized for $(m^z)^2 = 1$ whereas for $b > 0$ the vector \mathbf{m} is preferably orientated within the x - y plane with $m^z = 0$. For both cases, Eqs. (31) reduce to the two dimensional Laplace equation $\nabla^2 \Psi(\mathbf{x}) = 0$. This equation allows for topological defect solutions with $\Psi(x, y) = \arctan(y/x)$. In the top of Figs. 7 and 8 the spin distribution around isolated defects is shown for both $b < 0$ and $b > 0$. Using Eq. (32) one finds that the energy of a topological defect solution $\Psi(x, y)$ diverges logarithmically with the linear system size R ,

$$\beta E = \frac{1 + (m^z)^2 b}{2t_s} \pi \ln R. \quad (33)$$

Because of this logarithmic divergence of the energy, isolated defects are not present in absence of disorder and at sufficiently low temperatures. It can also be shown,⁴³ that a bound state of defect pairs, described by $g = g_{s1} g_{s2}$ with $g_{s1,2} = \exp\left[\frac{i}{2} \mathbf{m}_{1,2} \cdot \boldsymbol{\sigma} \arctan\left(\frac{y-y_{1,2}}{x-x_{1,2}}\right)\right]$, has a finite energy if $\mathbf{m}_1 + \mathbf{m}_2 = 0$. Therefore, while isolated defects may be absent, defect pairs will be present at any finite temperature. Figs. 7 and 8 (bottom) show such a pair of topological defects for $b < 0$ and $b > 0$, respectively.

This situation is reminiscent of the one encountered in the XY model where at low temperatures also only defect pairs are present. The pairs unbind at the critical Kosterlitz-Thouless temperature. An unbinding of defects at a critical temperature or critical disorder strength is also expected in the present model. The topological defects of the spiral differ however in important aspects from those of the XY model. Spiral defects have a Z_2

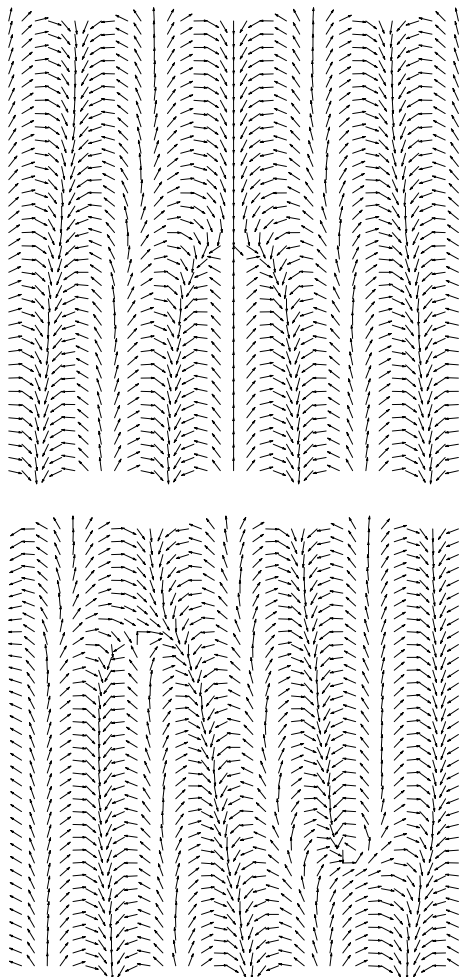


FIG. 7: Single topological defect (top) and topological defect pair (bottom) of a spiral with $b \leq 0$ (small scale AF fluctuations are not shown).

charge while XY defects have Z charges. More importantly, as the present model possesses asymptotic freedom, it has a finite correlation length ξ at any finite temperature even in absence of free defects. This implies that the logarithmic divergence in Eq. (33) appears only up to a scale $R < \xi$. It is therefore not clear how a defect-unbinding would affect the system. A transition from a phase with algebraically decaying spin correlations to a phase which shows an exponential decay, as occurs in XY models, is clearly ruled out. While in XY models topological defects can be relatively easily incorporated into the analysis because they can be decoupled from the spin waves, this is not the case for frustrated Heisenberg models. If fluctuations around the saddle point solution are taken into account, the defects of spirals couple to the spin waves already at second order in an expansion in the fluctuations³⁹. These difficulties have to date prevented a good understanding of defect unbinding in frustrated systems.

A comparison to XY models is nonetheless quite illu-

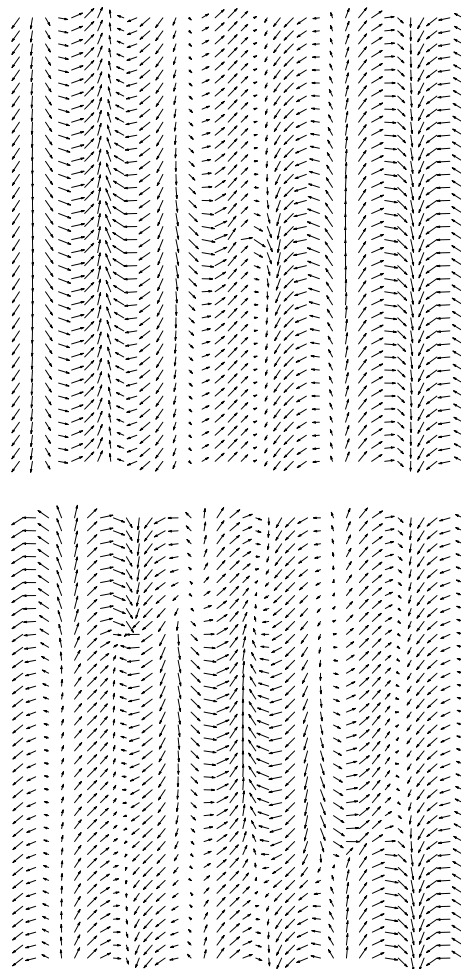


FIG. 8: Single topological defect (top) and topological defect pair (bottom) of a spiral with $b \geq 0$ (small scale AF fluctuations are not shown).

minating. The kind of disorder coupling we have used for the spiral phase is closely related in spirit to XY models with randomly fluctuating phases, where the disorder is also introduced in the form of a fluctuating gauge.⁴⁴ If one ignores vortices, the influence of the disorder was shown to amount to a simple renormalization of the spin stiffness, at all orders in a perturbative treatment of the disorder coupling^{44,45} and no disordering transition as a function of the disorder strength is found. However, once topological defects are included in the analysis, the coupling of vortices to the random gauge field can lead to a disordered phase even at $T = 0$. This transition is driven by the creation of unpaired defects if the fluctuations of the gauge field are stronger than some critical value.^{44,46} The critical disorder strength beyond which such defects appear can be estimated quite accurately when one calculates the free energy of an isolated defect in presence of disorder.^{44,47} It turns out that a similar analysis of a single defect in a spiral in presence of disorder can be carried out with some modifications, at least at the level

of saddle point solutions. Within this approximation, the free energy of an isolated spiral defect is given by

$$\beta F = \frac{1 + (m^z)^2 b}{2t_s} \pi \ln R - [\ln Z_d]_D, \quad (34)$$

where the second term contains the corrections due to the disorder coupling,

$$Z_d = \int d^2 \mathbf{y} \exp \left(-2 \int d^2 \mathbf{x} p_k \epsilon_{ijk} \epsilon_{abc} A_\mu^i n_j^a n_k^c Q_\mu^b \right) \quad (35)$$

with \mathbf{A}_μ , \mathbf{n}_k obtained from Eqs. (15), (16) and (30). With use of the replica trick $[\ln Z_d]_D = \lim_{N \rightarrow 0} \frac{1}{N} \ln [Z_d^N]_D$, we have, assuming $b < 0$,

$$[Z_d^N]_D = \int d^2 \mathbf{y}_1 \dots d^2 \mathbf{y}_N \exp \left(2\lambda p_1^2 \sum_{n, n'=1}^N \int d^2 \mathbf{x} \partial_\mu \Psi_n \partial_\mu \Psi_{n'} \right);$$

with $\Psi_n(\mathbf{x}) = \Psi(\mathbf{x} - \mathbf{y}_n)$. We write

$$\int d^2 \mathbf{x} \partial_\mu \Psi_n \partial_\mu \Psi_{n'} = -\frac{1}{2} \Delta_{nn'} + V^2, \quad (36)$$

with $V^2 \simeq 2\pi \ln R$ and $\Delta_{nn'} \simeq 4\pi \ln |\mathbf{y}_n - \mathbf{y}_{n'}|$.⁴⁶ For large separations $|\mathbf{y}_n - \mathbf{y}_{n'}|$ we approximate $\Delta_{nn'} \simeq 4\pi \ln R$ while for small distances $\Delta_{nn'}$ is negligible. To find the highest weight configuration, the replicas are grouped together in N/m sets containing each m replicas, with small distances between replicas within a set and large distance for replicas in different sets. $[Z_d^N]_D$ then scales with R as

$$[Z_d^N]_D \sim R^{4\lambda p_1^2 N^2 + \max_m (2\frac{N}{m} - 4\pi \lambda p_1^2 N(N-m))}. \quad (37)$$

In the limit $N \rightarrow 0$, maximization is replaced by minimization with respect to m in the range $0 \leq m \leq 1$, so

$$\beta F = [2p_1 \pi - \min_{0 \leq m \leq 1} (2/m + 4\lambda p_1^2 \pi m)] \ln R. \quad (38)$$

For $2\lambda p_1^2 \pi < 1$ one finds $\beta F = 2[p_1 \pi(1 - 2\lambda p_1) - 1] \ln R$ so that for $p_1 \pi(1 - 2\lambda p_1) \leq 1$ free defects are favorable. This is the phase boundary for thermal creation of defects. At low temperatures, $2\lambda p_1^2 \pi > 1$, one obtains $\beta F = 2\pi p_1(1 - \sqrt{8\lambda/\pi}) \ln R$ and a critical disorder strength $\lambda_c = \pi/8$ beyond which the disorder favors isolated defects even at $T = 0$. Similar considerations for the case $b \geq 0$ lead to the same critical disorder strength and the condition $\pi(p_1 + p_3)[1 - \lambda(p_1 + p_3)] \leq 2$ for thermal creation of free defects.

Let us first discuss the results for the disorder free case $\lambda = 0$. The situation is summarized in Fig. 9, which shows the line separating the regime where free vortices exist from the regime in which all defects are bound. Notice that the unbinding temperature goes linearly to zero in the limit $b \rightarrow -1$. At $b = -1$, free defects are present

at any finite temperature. This is expected, as at $b = -1$ and finite t_s , the topological defects we discuss here lose their meaning as the stiffness for rotations around the collinear ordering axis disappears and the model becomes a $O(3)/O(2)$ model which has no finite temperature transition. Whether or not free defects are present exactly at the point $b = -1$, $t_s = 0$ depends on how this point is approached. To see this, we note that the symmetry of the model in the limit $p_3 \rightarrow \infty$ but finite p_1 reduces to an XY symmetry as fluctuations of the \mathbf{n}_3 vector get suppressed which forces all fluctuations of the orthonormal pair $\mathbf{n}_{1,2}$ to lie within a plane. Therefore one obtains an XY model with stiffness p_1 . In terms of the b, t_s parameters, this limit is approached as $t_s \rightarrow 0$ and $b \rightarrow -1$ with finite $(1+b)/t_s = 4p_1$. Thus, depending on whether one approaches the point $1+b = t_s = 0$ with a slope larger or smaller than the critical one given by $(1+b)/t_s = 4/\pi$, one arrives at the disordered phase or the ordered phase of the XY model. This behavior is correctly reproduced by the free energy argument. The validity of the critical curve $(1+b)/t_s = 4/\pi$ also for finite $1+b > 0$ is at least plausible, as topological defect solutions also survive in this limit. Below this line, the RG Eqs. (20, 21) hold and the system should scale towards the point $b = 0$. We can only speculate however what happens above that line. At least for some finite regime near $b = -1$ the unbinding transition would presumably drive p_1 to zero, as it does in the XY model, and affect the renormalization of p_3 only weakly. Thus, the appearance of free defects will probably modify the RG equations at high temperatures in such a way that the system will flow back to the collinear point $b = -1$ as long as $1+b$ remains small enough. For larger b the nature of the RG is unclear. Numerical simulations on triangular Heisenberg models^{48,49} have found however clear evidence for a defect unbinding transition. As the triangular Heisenberg model is believed to have initially $b = 1$,³⁵ it is likely that an unbinding transition indeed occurs for every initial value of b . As no RG equations are available which can describe the transition, the form of the correlation length near this transition is unknown. It was however argued³⁹ that the temperature dependence of the correlation length should cross over from the NL σ M behavior to an XY behavior when the defects unbind. Numerical results seem to support such a scenario.⁴²

Let us now turn to the case with disorder. Disorder will lead to the formation of free defects if $\lambda > \pi/8$. According to the free energy argument above, this critical disorder strength is independent of the stiffnesses p_k and is thus also valid in the XY limit discussed above. For strong enough disorder, free topological defects will exist already at $T = 0$, invalidating our NL σ M analysis and producing very short low-temperature correlation lengths for the spiral. For XY models, the correlation length at $T = 0$ behaves like $\xi \propto \exp(B/\sqrt{\lambda - \lambda_c})$ (with some constant B) near the critical disorder strength.⁴⁴ This form of the correlation length has a divergence of ξ at $\lambda = \lambda_c$ which cannot be correct for the spiral because, as

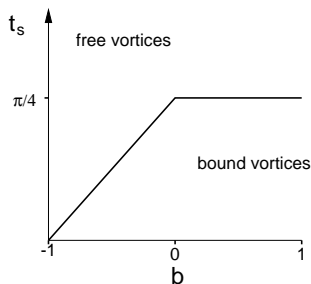


FIG. 9: The critical line for the thermal unbinding of topological defects is shown in b, t_s space.

discussed above, even without vortices, the coupling of any finite amount of disorder to the spins will lead to a finite correlation length. The correct dependence of the correlation length at $T = 0$ on the disorder is expected to be an interpolation between the $NL\sigma M$ result and the XY behavior.

Certainly, the free energy argument is not expected to work as well in the present model as it does for XY models. The parameters λ and t_s flow to strong coupling and thus the predictions of the free energy argument also become scale dependent. In other words, while at some small scale the system might look stable against the creation of free defects, at some larger scale the system will become unstable according to the free energy argument. There does not seem to be a simple answer as to which scale is the correct one for applying the argument. Note that such problems do not arise in the XY model where the stiffness remains unchanged under the RG as long as vortices are ignored. In view of the divergence of the λ and t_s parameters in the $NL\sigma M$, one possible scenario would be that free defects will always be present at sufficiently large length scales. Numerical results do however not support such a scenario and rather point to the existence of a finite critical temperature.⁴⁹ Below we shall apply the free energy argument with the bare parameters, i.e. at the smallest possible scale, which, if anything, would overestimate the stability of the system against free defect formation.

IV. COMPARISON WITH EXPERIMENTS

Let us now compare our results with experimental data on the SG phase of $\text{La}_{2-x}\text{Sr}_x\text{CuO}_4$. Neutron scattering data¹⁶ have revealed an incommensurability of the spins which scales roughly linearly with x . At very small x , a small deviation from the linear dependence is observed. Both features can be explained within the dipole model. The linear scaling is reproduced if the fraction of the dipoles which are ordered is doping independent, i.e., the number of ordered dipoles scales linearly with doping. The deviation from linearity might be explained with the increase of the average separation between dipoles

at small x and a resulting diminished tendency of the dipoles to align.

The same experimental data also shows the strong one dimensional character of the IC modulation, i.e. the incommensurability is observed only in one diagonal of the Cu-lattice (b -direction) and thus breaks the symmetry of the square lattice. This phenomenon is usually interpreted as being due to the existence of charge and spin stripes running along the other diagonal (a -direction). However, this IC is also expected for a spiral along the b -direction because its chirality breaks the translation symmetry (it can spiral clock- or anticlock-wise). In addition, this symmetry breaking is expected to show long-range order because the dipoles prefer a discrete set of lattice orientations.

Another important consequence of the spiral chirality is the formation of topological defects. To judge, whether or not topological defects play a role in the LSCO SG phase, we need an estimate of λ . We can use as a lower bound for λ the result obtained from the collinear analysis²⁴ where a disorder parameter equivalent to ours, but defined on the much smaller scale of the AF unit cell, was used. From a fit of the x dependence of the correlation length at $x < 0.02$ and large temperatures $T > T_N$, one obtains $\lambda \simeq 20x$. In this regime of x , the low temperature phase has long-range AF order and a collinear analysis is well justified. We assume that the linear dependence of the disorder parameter on x , $\lambda \simeq 20x$, also holds in the SG regime. This view is supported by measurements, which found that the width of the distribution of internal magnetic fields (i.e. local staggered moments) increases simply linearly with doping, with no detectable change on crossing the AF/SG phase boundary,¹⁰ see also Fig. 1. It is remarkable that with our above estimate for the critical disorder strength $\lambda_c = \pi/8$ we find a critical doping concentration $x_c \sim 0.02$. Considering that $\lambda \simeq 20x$ is a conservative lower bound of λ at the long length scales relevant to spirals, we conclude that in the entire SG phase, free topological defects will be present already at $T = 0$, leading to a strongly disordered spiral phase. Experiments have in fact shown that the correlation lengths in the SG regime are rather short and of the same order as the periodicity of the IC modulation.¹⁶ While this is in accordance with the expected presence of topological defects, the correlation lengths are so short that the condition $\xi \gg |\mathbf{q}_s|^{-1}$ is not fulfilled. The regime where spiral correlations become dominant is therefore barely reached, and the RG scaling predictions cannot be well tested.

While qualitatively the experimental data supports a description of the SG phase as a strongly disordered spiral state, both the extremely short correlation lengths and our limited understanding of topological defects prevent a more quantitative comparison.

However, our suggestion that the incommensurability of the spins is related to ordered dipolar frustration centers can be directly tested experimentally on co-doped samples $\text{La}_{2-x}\text{Sr}_x\text{Zn}_z\text{Cu}_{1-z}\text{O}_4$. Zn replaces Cu in the

CuO₂ planes and effectively removes one spin. Zn doping leads therefore to a dilution of the AF but does not introduce frustration. Dilution is not very effective in destroying the AF order and pure Zn doping (with $x = 0$) leads to a destruction of long-range order only at percolation threshold that occurs for $x \approx 41\%$.⁵⁰ Surprisingly, for very small Sr concentration $x \leq 0.02$ it was found that co-doping with Zn can increase T_N .⁵¹ This is remarkable as both kinds of impurities lead to a reduction of T_N in singly doped samples. A possible explanation for this behavior was suggested by Korenblit *et al.*⁵² They put forward an argument, that Zn impurities, if placed close enough to the localized hole state, will destroy the frustrating nature of the hole bound state. While their microscopic picture of frustration is a classical one, a Zn impurity is also expected to strongly influence the properties of the bound hole state within a more realistic quantum mechanical picture of frustration. Although Zn couples only weakly to the spin degrees of freedom, if placed near a Sr donor, it disturbs the symmetry around the Sr atom and modifies the nature of the bound hole state. As the Zn impurity breaks the sublattice pseudo-spin degeneracy of the bound hole, the orientation of the dipole moment is no longer annealed but becomes quenched. Another effect of the breaking of the sublattice symmetry is that the weight of the bound hole wave function near the wavevector $(\pi/2, \pi/2)$ or equivalent points will be reduced. As it is these wavevectors which are responsible for frustrating the spin background, one would expect a reduction or possibly a complete destruction of the frustration caused by the hole. Hence, the effective density of dipoles will be renormalized to $x \rightarrow x(1-\gamma z)$ where γ must be calculated from a microscopic theory (experiments indicate that γ is of order 2).⁵² Co-doping with Zn then has two effects: First, it lowers the amount of frustration in the sample and thus increases the correlation length, which would explain the experimentally observed increase of T_N with z for $x = 0.017$.^{51,52} Furthermore, the effect of quenching the dipole moments will be the same as destroying them altogether with respect to the incommensurability, as the incommensurability is determined solely by the ordered moments. Thus, co-doping with Zn will lead to a decrease of the incommensurability by a factor $1 - \gamma z$. In contrast, within a stripe picture, co-doping with Zn is not expected to change the incommensurability as the hole density is not affected by Zn doping. Previous measurements in the superconducting phase ($x = 0.12$ and $x = 0.14$), where the stripe model is believed to be valid, have shown that the incommensurability indeed remains intact upon co-doping with Zn.^{53,54,55} Within a stripe picture, the only effect of Zn co-doping in the SG regime should be pinning of stripes, which would lead to a reduced correlation length.⁵⁶ Therefore, neutron scattering experiments within the SG regime of Zn co-doped samples could clarify the debate, if the magnetic incommensurability observed in the SG regime is to be interpreted within a stripe or a frustration based model.

It is interesting that symmetry arguments similar to

those just used to discuss Zn co-doping also give a simple explanation for the absence of any incommensurate signal in Li doped La₂Cu_{1-y}Li_yO₄. For small y , these compounds show a magnetic phase diagram which is almost identical to Sr doped samples⁵⁷ with the notable exception that the magnetic correlations always remain commensurate.⁵⁸ Like Sr, each Li atom introduces an excess hole in the CuO₂ plane which, at least for small doping concentrations, remains weakly localized to its dopant. The important difference is that Li replaces Cu in the crystal and thus has a different symmetry with respect to the magnetic sublattice ordering than a Sr hole. Specifically, the sublattice position of the Li atom breaks the pseudospin degeneracy present in Sr doped samples. Assuming that otherwise the origin of frustration is the same, the only difference between Sr and Li doped samples is that the dipole moment assigned to the Li bound hole is quenched, whereas the one of the Sr hole is annealed. Thus, ordering of these moments and the development of incommensurate correlations cannot occur in Li doped samples.

In conclusion, we have presented a detail picture of the dipole model of frustration and discussed its applicability to the weakly doped regime of cuprate materials. Most of the key characteristics of these materials were already known to be in accordance with the model and we showed that incommensurate correlations appear also naturally within the dipole picture. We extended the commensurate model to allow for a description of the resulting disordered spiral spin phases. Finally, we suggested an experiment which would allow to verify whether the frustration based dipole model or the stripe picture is realized within the weakly doped regime of cuprates.

V. ACKNOWLEDGMENTS

We acknowledge fruitful discussions with V. Gritsev, V. Juricic, B. Normand, and B. Simovic. C. M. S. is supported by the Swiss National Foundation under grant 620-62868.00.

APPENDIX A: SU(2) REPRESENTATION

The orthonormal basis \mathbf{n}_k can be related to an element g of $SU(2)$ through $g\sigma^k g^{-1} = \mathbf{n}_k \cdot \boldsymbol{\sigma}$, or

$$n_k^a = \frac{1}{2} \text{tr} \{ \sigma^a g \sigma^k g^{-1} \} \quad (\text{A1})$$

For the derivative one finds, using $\partial_\mu (g g^{-1}) = 0$,

$$\begin{aligned} \partial_\mu n_k^a &= \frac{1}{2} \text{tr} \{ \sigma^a \partial_\mu g \sigma^k g^{-1} + \sigma^a g \sigma^k \partial_\mu g^{-1} \} \\ &= \frac{1}{2} \text{tr} \{ \sigma^k [g^{-1} \sigma^a g, g^{-1} \partial_\mu g] \}. \end{aligned} \quad (\text{A2})$$

Introducing $g^{-1}\partial_\mu g = i\mathbf{A}_\mu \cdot \boldsymbol{\sigma}$ and with $[\sigma^i, \sigma^j] = 2i\epsilon_{ijk}\sigma^k$ one finds

$$\partial_\mu n_k^a = 2\epsilon_{ijk}A_\mu^i n_j^a. \quad (\text{A3})$$

Therefore, we have (with $p_{1\mu} = p_{2\mu}$)

$$\begin{aligned} p_{k\mu}(\partial_\mu \mathbf{n}_k)^2 &= 4p_{k\mu}(\epsilon_{ijk}A_\mu^i n_j^a)^2 = 4p_{k\mu}(\epsilon_{ijk})^2 (A_\mu^k)^2 \\ &= \frac{2}{t_\mu} \left[\mathbf{A}_\mu^2 + b(A_\mu^z)^2 \right], \end{aligned} \quad (\text{A4})$$

with $t_\mu^{-1} = 2(p_{1\mu} + p_{3\mu})$ and $bt_\mu^{-1} = 2(p_{1\mu} - p_{3\mu})$.

APPENDIX B: EXPANDING THE ENERGY FUNCTIONAL IN φ^i

To do the RG, we introduce $g = \tilde{g} \exp(i\boldsymbol{\varphi} \cdot \boldsymbol{\sigma})$, where φ^a are fast fields fluctuating with wavelengths $[\Lambda^{-1}, 1]$ and \tilde{g} has only slow fluctuations in the range $[0, \Lambda^{-1}]$. For the 1-loop calculation, we need to expand \mathbf{n}_k and A_μ^k up to second order in φ^a . We then find

$$\begin{aligned} n_i^a &= \frac{1}{2} \text{tr} \left\{ \sigma^a \tilde{g} \exp(i\boldsymbol{\varphi} \cdot \boldsymbol{\sigma}) \sigma^i \exp(-i\boldsymbol{\varphi} \cdot \boldsymbol{\sigma}) \tilde{g}^{-1} \right\} \\ &= \tilde{n}_i^a + \frac{i}{2} \text{tr} \left\{ \sigma^a \tilde{g} [\boldsymbol{\varphi} \cdot \boldsymbol{\sigma}, \sigma^i] \tilde{g}^{-1} \right\} \\ &+ \frac{1}{2} \text{tr} \left\{ \sigma^a \tilde{g} \left(\boldsymbol{\varphi} \cdot \boldsymbol{\sigma} \sigma^i \boldsymbol{\varphi} \cdot \boldsymbol{\sigma} - \frac{1}{2} (\boldsymbol{\varphi} \cdot \boldsymbol{\sigma})^2 \sigma^i \right. \right. \\ &\left. \left. - \frac{1}{2} \sigma^i (\boldsymbol{\varphi} \cdot \boldsymbol{\sigma})^2 \right) \tilde{g}^{-1} \right\} + \mathcal{O}(\varphi^3) \\ &= \tilde{n}_i^a + 2\epsilon_{ijk} \varphi^j \tilde{n}_k^a + \varphi^j \varphi^k R_{jk}^{ai} + \mathcal{O}(\varphi^3), \end{aligned} \quad (\text{B1})$$

where

$$R_{jk}^{ai} = \frac{1}{2} \text{tr} \left\{ \sigma^a \tilde{g} \left(\sigma^j \sigma^i \sigma^k - \frac{1}{2} \sigma^j \sigma^k \sigma^i - \frac{1}{2} \sigma^i \sigma^j \sigma^k \right) \tilde{g}^{-1} \right\}.$$

It turns out, that in the RG we will only need the diagonal components of R_{jk}^{ai} with $j = k$ which have the much simpler form $R_{zz}^{ai} = -2(\epsilon_{zqi})^2 \tilde{n}_i^a$ (we put here $j = k = z$ to make clear that z is not a silent index, the equation also holds for $j = x, y$). Similarly, we find

$$\begin{aligned} A_\mu^i &= \frac{1}{2i} \text{tr} \left\{ \sigma^i \exp(-i\boldsymbol{\varphi} \cdot \boldsymbol{\sigma}) [\partial_\mu + \tilde{g}^{-1} \partial_\mu \tilde{g}] \exp(i\boldsymbol{\varphi} \cdot \boldsymbol{\sigma}) \right\} \\ &= \tilde{A}_\mu^i + \frac{1}{2} \text{tr} \left\{ \sigma^i \left(\partial_\mu \boldsymbol{\varphi} \cdot \boldsymbol{\sigma} + \frac{1}{2i} [\boldsymbol{\varphi} \cdot \boldsymbol{\sigma}, \partial_\mu \boldsymbol{\varphi} \cdot \boldsymbol{\sigma}] \right. \right. \\ &+ i [\tilde{\mathbf{A}}_\mu \cdot \boldsymbol{\sigma}, \boldsymbol{\varphi} \cdot \boldsymbol{\sigma}] + \boldsymbol{\varphi} \cdot \boldsymbol{\sigma} \tilde{\mathbf{A}}_\mu \cdot \boldsymbol{\sigma} \boldsymbol{\varphi} \cdot \boldsymbol{\sigma} \\ &\left. \left. - \frac{1}{2} (\boldsymbol{\varphi} \cdot \boldsymbol{\sigma})^2 \tilde{\mathbf{A}}_\mu \cdot \boldsymbol{\sigma} - \frac{1}{2} \tilde{\mathbf{A}}_\mu \cdot \boldsymbol{\sigma} (\boldsymbol{\varphi} \cdot \boldsymbol{\sigma})^2 \right) \right\} + \mathcal{O}(\varphi^3) \\ &= \tilde{A}_\mu^i + \partial_\mu \varphi^i + \epsilon_{ijk} \varphi^j \partial_\mu \varphi^k + 2\epsilon_{ijk} \varphi^j \tilde{A}_\mu^k - 2\tilde{A}_\mu^i \varphi^2 \\ &+ 2\tilde{\mathbf{A}}_\mu \cdot \boldsymbol{\varphi} \varphi^i + \mathcal{O}(\varphi^3). \end{aligned} \quad (\text{B2})$$

APPENDIX C: PROPAGATOR OF THE φ^i FIELDS

As already mentioned, there is a small spatial anisotropy in the stiffnesses $p_{k\mu}$, i.e. $p_{k1} \neq p_{k2}$. We shall keep here the spatial dependence of the stiffnesses $p_{k\mu}$ up to first order in the anisotropy, assuming that the anisotropy κ , which we define through $p_{k1}/p_{k2} = 1 + \kappa$, is independent of the k index. Thus we can absorb the anisotropy into the t_μ parameter while b remains isotropic. We then define $t_s = \sqrt{t_1 t_2}$ and $t_{1,2} \simeq (1 \pm \kappa/2)t_s$. For future use, we also define the isotropic stiffnesses $p_k = \sqrt{p_{k1} p_{k2}}$. It is not clear whether the isotropy of b is preserved under the RG and we have made no attempt to write down the RG equations in presence of anisotropy. In principle, if b remains isotropic, the results obtained below allow to determine the flow of the anisotropy parameter κ under the RG. For possible future use, we will therefore keep the perturbative expansion with the anisotropy. The results used in the body of this work have however been obtained for an isotropic $t_\mu = t_s$, i.e. $\kappa = 0$.

We need to expand the exponential $\exp(-H_P)$ and integrate out the φ^i fields. Taking the average over the φ^i fields is done with the Gaussian term H_φ of Eq. (18). The propagator for the φ^i is thus quite simple and becomes, to lowest order in the anisotropy κ

$$\begin{aligned} C^i(\mathbf{x}) &:= \langle \varphi^i(\mathbf{x}) \varphi^i(\mathbf{0}) \rangle_\varphi = \frac{t_s}{2(1 + b\delta_{iz})} \int \frac{d^2 \mathbf{k}}{(2\pi)^2} \frac{e^{i\mathbf{k} \cdot \mathbf{x}}}{k^2} \\ &\left(1 + \kappa \frac{k_1^2 - k_2^2}{2k^2} \right) \times (\Upsilon(k, \Lambda) - \Upsilon(k, 1)). \end{aligned} \quad (\text{C1})$$

The IR cutoff is provided by the function $\Upsilon(k, \Lambda)$. A sharp cutoff, $\Upsilon(k, \Lambda) = \Theta(k - \Lambda^{-1})$ has the disadvantage of producing a long-ranged C^i and we therefore adopt instead $\Upsilon(k, \Lambda) = [1 + (k\Lambda)^{-2}]^{-1}$, which renders C^i short ranged.

In our RG calculation we will mainly need $C^i(\mathbf{0})$ which has the form

$$C^x(\mathbf{0}) = C^y(\mathbf{0}) = \frac{t_s}{4\pi} \ln \Lambda + \mathcal{O}(\kappa^2), \quad C^z(\mathbf{0}) = \frac{1}{1+b} C^x(\mathbf{0}).$$

Another useful formula is

$$t_\mu^{-1} \int d^2 \mathbf{x} (\partial_\mu C^x)^2 = \frac{1}{2} C^x(\mathbf{0}) + \mathcal{O}(\kappa^2). \quad (\text{C2})$$

APPENDIX D: RENORMALIZATION

We can immediately discard all terms of third or higher power in $\tilde{\mathbf{A}}_\mu$ as these terms are irrelevant in a RG sense. Terms second order in $\tilde{\mathbf{A}}_\mu$ renormalize t_μ and b , whereas terms linear in $\tilde{\mathbf{A}}_\mu$ are responsible for the renormalization of the disorder variance λ .

First, we note that the terms H_2, H_3 do not contribute to the renormalization, as was pointed out for the calculation of the RG for the disorder free system in Ref. [43].

This is because these terms are linear in φ while they do not involve a disorder field \mathbf{Q}_μ . For an abelian theory, such terms cannot contribute because the fast φ^i fields and the slow $\tilde{\mathbf{A}}_\mu$ fields have their support in orthogonal parts of the wave vector space. Here, for the non-abelian case, this argument is not sufficient because the $\tilde{\mathbf{A}}_\mu$ fields are not linearly related to the fields g . For the present non-abelian theory this is nonetheless true, although an explicit calculation is required to see this. For example, H_2^2 does not contribute, because its contribution is built from terms of the form (we omit the upper i indices of C^i and A_μ^i here for simplicity)

$$\int d^2\mathbf{x} \int d^2\mathbf{x}' \tilde{A}_\mu(\mathbf{x}) \tilde{A}_{\mu'}(\mathbf{x}') \partial_\mu \partial_{\mu'} C(\mathbf{x} - \mathbf{x}') \quad (\text{D1})$$

To evaluate this term, we change to center of mass (\mathbf{y}) and relative (\mathbf{y}') coordinates and then perform a gradient expansion in the relative coordinate. Only the lowest order contribution is of interest, as higher order terms involve a local coupling of the type $A_\mu(\partial_\nu)^n A_{\mu'}$ with $n > 0$ which are irrelevant from a scaling point of view.

The lowest order term is then

$$- \int d^2\mathbf{y} \tilde{A}_\mu(\mathbf{y}) \tilde{A}_{\mu'}(\mathbf{y}) \int d^2\mathbf{y}' \partial_\mu \partial_{\mu'} C(\mathbf{y}') \quad (\text{D2})$$

which vanishes because the last integral is zero. In the following we will omit H_2 and H_3 from the analysis, because terms involving them do not contribute. This can be shown for each term in a way similar to the one just shown.

We want to find the RG equations up to second order in t_μ and λ . In the n th order of the cumulant expansion of \mathcal{F} , Eq. (19), we only need to consider terms which have a total number of φ and \mathbf{Q}_μ fields less than $2n + 2$. This is because each term of order n carries a factor t_s^{-n} from the prefactors of the terms in H_p and each pair of $\varphi(\mathbf{Q}_\mu)$ produces a factor $t_s(\lambda)$.

We begin first with the terms renormalizing t_μ and b , where we give a detailed calculation only for the terms up to second order in H_p . The calculation of higher order terms is quite lengthy although conceptually easy and we therefore just present the results of the calculation.

1. Terms which renormalize t_μ and b

a. First order in H_p

There is only one term quadratic in $\tilde{\mathbf{A}}_\mu$ which contributes, H_4 (the φ^i average over H_3 is zero).

$$\begin{aligned} - \langle H_4 \rangle_{\varphi c} &= -4 \frac{b}{t_\mu} \int d^2\mathbf{x} \left[\epsilon_{zjk} \epsilon_{zj'k'} \tilde{A}_\mu^k \tilde{A}_{\mu'}^{k'} \langle \varphi^j \varphi^{j'} \rangle_\varphi - \left(\tilde{A}_\mu^z \right)^2 \langle \varphi^l \varphi^l \rangle_\varphi + \tilde{A}_\mu^z \tilde{A}_{\mu'}^l \langle \varphi^z \varphi^l \rangle_\varphi \right] \\ &= -4 \frac{b}{t_\mu} \int d^2\mathbf{x} \left[(\epsilon_{zjk})^2 \left(\tilde{A}_\mu^k \right)^2 C^j(\mathbf{0}) - \left(\tilde{A}_\mu^z \right)^2 \sum_l C^l(\mathbf{0}) + \left(\tilde{A}_\mu^z \right)^2 C^z(\mathbf{0}) \right] \\ &= -4b t_\mu^{-1} \int d^2\mathbf{x} \left[\tilde{\mathbf{A}}_\mu^2 - 3 \left(\tilde{A}_\mu^z \right)^2 \right] C^x(\mathbf{0}). \end{aligned} \quad (\text{D3})$$

b. Second order in H_p

Terms with odd numbers of φ^i or \mathbf{Q}_μ are zero after performing the φ^i and disorder average. There are then only two terms we need to consider, H_1^2 and H_{c1}^2 (H_{c3}^2 has a total of six φ^i and Q_μ^i fields and does not contribute and H_2 terms do not contribute as mentioned above). For H_1^2 we have

$$\begin{aligned} \frac{1}{2} \left[\langle H_1^2 \rangle_{\varphi c} \right]_D &= \frac{1}{2} \langle H_1^2 \rangle_{\varphi c} \\ &= 2t_\mu^{-1} t_{\mu'}^{-1} \int d^2\mathbf{x} d^2\mathbf{x}' \tilde{A}_\mu^i(\mathbf{x}) \tilde{A}_{\mu'}^{i'}(\mathbf{x}') \epsilon_{ijk} \epsilon_{i'j'k'} (1 - b\delta_{iz} + 2b\delta_{jz}) \\ &\quad \times (1 - b\delta_{i'z} + 2b\delta_{j'z}) \left\langle \partial_\mu \varphi^j(\mathbf{x}) \varphi^k(\mathbf{x}) \partial_{\mu'} \varphi^{j'}(\mathbf{x}') \varphi^{k'}(\mathbf{x}') \right\rangle_\varphi \end{aligned} \quad (\text{D4})$$

The four point average can be decomposed according to Wick's Theorem. Nonzero contributions arise from the contractions $\langle jk' \rangle \langle j'k \rangle$ and $\langle jj' \rangle \langle kk' \rangle$. We again employ an expansion of H_1^2 in the relative coordinate and keep only the zeroth order term of the expansion. This yields

$$\frac{1}{2} \langle H_1^2 \rangle_{\varphi c} \simeq 2t_\mu^{-2} \int d^2\mathbf{x} \tilde{A}_\mu^i \tilde{A}_{\mu'}^{i'} \epsilon_{ijk} \epsilon_{i'j'k'} (1 - b\delta_{iz} + 2b\delta_{jz}) (1 - b\delta_{i'z} + 2b\delta_{j'z})$$

$$\begin{aligned}
& \times (\delta_{jj'}\delta_{kk'} - \delta_{kj'}\delta_{jk'}) \int d^2\mathbf{y} \partial_\mu C^j(\mathbf{y}) \partial_\mu C^k(\mathbf{y}) \\
& = 4t_\mu^{-2} \int d^2\mathbf{x} \left(\tilde{A}_\mu^i \right)^2 (\epsilon_{ijk})^2 (1 - b\delta_{iz} + 2b\delta_{jz}) (1 - b\delta_{iz} + b\delta_{jz} + b\delta_{kz}) \\
& \times \int d^2\mathbf{y} \partial_\mu C^j(\mathbf{y}) \partial_\mu C^k(\mathbf{y}).
\end{aligned} \tag{D5}$$

With use of Eq. (C2), we finally find

$$\frac{1}{2} \langle H_1^2 \rangle_{\varphi c} = 2t_\mu^{-1} \int d^2\mathbf{x} \left[\tilde{\mathbf{A}}_\mu^2 (1+b) + \left(\tilde{A}_\mu^z \right)^2 b(b-3) \right] C^x(\mathbf{0}) \tag{D6}$$

The other second order contribution is

$$\begin{aligned}
\frac{1}{2} \left[\langle H_{c1}^2 \rangle_{\varphi c} \right]_D & = 8 \int d^2\mathbf{x} d^2\mathbf{x}' p_{k\mu} p_{k'\mu'} \epsilon_{ijk} \epsilon_{i'j'k'} \epsilon_{abc} \epsilon_{a'b'c'} \left\{ \epsilon_{klm} \tilde{n}_j^a \tilde{n}_m^c \tilde{A}_\mu^i \right. \\
& \quad \left. + \epsilon_{jlm} \tilde{n}_k^c \tilde{n}_m^a \tilde{A}_\mu^i + \epsilon_{ilm} \tilde{n}_j^a \tilde{n}_k^c \tilde{A}_\mu^m \right\} \left\{ \epsilon_{k'l'm'} \tilde{n}_{j'}^{a'} \tilde{n}_{m'}^{c'} \tilde{A}_{\mu'}^{i'} + \epsilon_{j'l'm'} \tilde{n}_{k'}^{c'} \tilde{n}_{m'}^{a'} \tilde{A}_{\mu'}^{i'} \right. \\
& \quad \left. + \epsilon_{i'l'm'} \tilde{n}_{j'}^{a'} \tilde{n}_{k'}^{c'} \tilde{A}_{\mu'}^{m'} \right\} \delta_{ll'} C^l(\mathbf{x} - \mathbf{x}') \left[Q_\mu^b(\mathbf{x}) Q_{\mu'}^{b'}(\mathbf{x}') \right]_D.
\end{aligned} \tag{D7}$$

Using $\left[Q_\mu^b(\mathbf{x}) Q_{\mu'}^{b'}(\mathbf{x}') \right]_D = \delta_{bb'} \delta_{\mu\mu'} \delta(\mathbf{x} - \mathbf{x}') \lambda$, $\epsilon_{abc} \epsilon_{a'bc'} = \delta_{aa'} \delta_{cc'} - \delta_{ac'} \delta_{ca'}$ and the orthonormality of the \mathbf{n}_k , we find after some algebra

$$\frac{1}{2} \left[\langle H_{c1}^2 \rangle_{\varphi c} \right]_D = 2\lambda b^2 t_\mu^{-2} \int d^2\mathbf{x} \left[\tilde{\mathbf{A}}_\mu^2 + \left(\tilde{A}_\mu^z \right)^2 \right] C^x(\mathbf{0}). \tag{D8}$$

Higher order terms can be evaluated in much the same way as the first and second order terms, although the large number of indices makes their evaluation more tedious. We therefore refrain here from a detailed presentation of these terms and just state the results.

c. Third order in H_p

Terms of second order in $\tilde{\mathbf{A}}_\mu^2$ are produced by $(H_1 + H_{c1} + H_{c3})^2 (H_{c2} + H_{c4})$. However, only the terms $H_1(H_{c1} + H_{c3})(H_{c2} + H_{c4})$ have even powers of \mathbf{Q}_μ . Terms with eight or more φ and \mathbf{Q}_μ fields again do not contribute to second order in λ, t_μ . Thus we are left with only $H_1 H_{c1} H_{c2}$. We find

$$- \left[\langle H_1 H_{c1} H_{c2} \rangle_{\varphi c} \right]_D = -2\lambda t_\mu^{-2} b \int d^2\mathbf{x} \left[\tilde{\mathbf{A}}_\mu^2 (1+b) + \left(\tilde{A}_\mu^z \right)^2 (b-3) \right] C^x(\mathbf{0}). \tag{D9}$$

We further need to consider terms of the type $(H_{c2} + H_{c4})^2 H_4$. Only $H_{c2}^2 H_4$ has less than eight φ, \mathbf{Q}_μ fields and even powers of both fields. We find

$$- \frac{1}{2} \left[\langle H_{c2}^2 H_4 \rangle_{\varphi c} \right]_D = -2\lambda b t_s^{-1} t_\mu^{-1} \int d^2\mathbf{x} \left[\tilde{\mathbf{A}}_\mu^2 - 3 \left(\tilde{A}_\mu^z \right)^2 \right] C^x(\mathbf{0}). \tag{D10}$$

d. Fourth order in H_p

Possible contributions arise from the terms $(H_1 + H_{c1} + H_{c3})^2 (H_{c2} + H_{c4})^2$. Discarding terms with ten or more $\varphi^i, \mathbf{Q}_\mu$ fields, we are left with $H_{c2}^2 H_1^2$ and $H_{c2}^2 H_{c1}^2$. However, the connected part of the φ^i average of $H_{c2}^2 H_{c1}^2$ is zero (its finite disconnected parts enter the renormalization of the disorder, see below), and the only contribution is therefore

$$\frac{1}{4} \left[\langle H_{c2}^2 H_1^2 \rangle_{\varphi c} \right]_D = \lambda t_s^{-1} t_\mu^{-1} \int d^2\mathbf{x} \left[\tilde{\mathbf{A}}_\mu^2 (2+b)(1+b) + \left(\tilde{A}_\mu^z \right)^2 b(b-7) \right] C^x(\mathbf{0}). \tag{D11}$$

Terms of the form $H_4(H_{c2} + H_{c4})^3$ do not contribute because their disorder average is zero. Higher order terms in H_p do not contribute because they either involve more than four \mathbf{Q}_μ terms and are therefore of higher order than λ^2 or they do not contain finite connected parts. For example, the term $\langle H_4 H_{c2}^4 \rangle_{\varphi c}$ decomposes into products of averages of $\langle H_4 \rangle_{\varphi c}$ or $\langle H_4 H_{c2}^2 \rangle_{\varphi c}$ and $\langle H_{c2}^2 \rangle_{\varphi c}$.

2. Terms which renormalize λ

linear in \tilde{A}_μ^i . We list the contributions order by order

To find the renormalization of the variance of the disorder distribution, we first collect all connected terms

below.

c. Third order in H_p

a. First order in H_p

Only three terms are linear in \tilde{A}_μ^i , H_1 , H_{c1} and H_{c3} . However, both H_1 and H_{c1} have a zero φ^i average and only $\langle H_{c3} \rangle_{\varphi c}$ contributes.

There are contributions from $\langle H_{c1}H_{c2}H_{c4} \rangle_{\varphi c}$, $\langle H_{c3}H_{c2}^2 \rangle_{\varphi c}$ and $\langle H_1H_{c2}^2 \rangle_{\varphi c}$. The terms $\langle H_{c3}H_{c4}^2 \rangle_{\varphi c}$ and $\langle H_1H_{c4}^2 \rangle_{\varphi c}$ do not contribute, as they contain eight or more Q_μ^i , φ^i fields.

b. Second order in H_p

At second order there are contributions from $\langle H_{c1}H_{c2} \rangle_{\varphi c}$ and $\langle H_1H_{c4} \rangle_{\varphi c}$. There is no contribution to second order in λ , t_μ of the disorder renormalization from $\langle H_{c3}H_{c4} \rangle_{\varphi c}$ because this term has six Q_μ^i , φ^i .

d. Fourth order in H_p

Only one term contributes, $\langle H_1H_{c2}^2H_{c4} \rangle_{\varphi c}$. All other terms have ten or more Q_μ^i , φ^i fields or more than three \mathbf{Q}_μ fields and thus do not contribute. The same argument applies to all terms generated by higher order of H_p .

3. Calculating the renormalized disorder variance

We now must calculate the variance of all terms at the new length scale Λ^{-1} which are linear in \tilde{A}_μ^i . These are the terms just found above plus H_{c0} . Thus, we need to calculate the variance of

$$\begin{aligned} & -H_{c0} - \langle H_{c3} \rangle_{\varphi c} + \langle H_{c1}H_{c2} \rangle_{\varphi c} + \langle H_1H_{c4} \rangle_{\varphi c} - \langle H_{c1}H_{c2}H_{c4} \rangle_{\varphi c} - \frac{1}{2} \langle H_{c2}^2H_{c3} \rangle_{\varphi c} \\ & - \frac{1}{2} \langle H_{c2}^2H_1 \rangle_{\varphi c} + \frac{1}{2} \langle H_1H_{c2}^2H_{c4} \rangle_{\varphi c} \end{aligned} \quad (\text{D12})$$

To order λ^2 , the following terms contribute to the variance.

$$\begin{aligned} [H_{c0}^2]_D &= \lambda t_\mu^{-2} \int d^2\mathbf{x} \left\{ \left[\left(\tilde{A}_\mu^x \right)^2 + \left(\tilde{A}_\mu^y \right)^2 \right] + \left(\tilde{A}_\mu^z \right)^2 (1+b)^2 \right\}, \\ 2 \left[\langle H_{c3} \rangle_{\varphi c} H_{c0} \right]_D &= 8\lambda t_\mu^{-2} \int d^2\mathbf{x} \left\{ \left[\left(\tilde{A}_\mu^x \right)^2 + \left(\tilde{A}_\mu^y \right)^2 \right] b \right. \\ & \quad \left. - \left(\tilde{A}_\mu^z \right)^2 2b(1+b) \right\} C^x(\mathbf{0}), \\ -2 \left[\langle H_1H_{c4} \rangle_{\varphi c} H_{c0} \right]_D &= -4\lambda t_\mu^{-2} \int d^2\mathbf{x} \left\{ \left[\left(\tilde{A}_\mu^x \right)^2 + \left(\tilde{A}_\mu^y \right)^2 \right] (1+b) \right. \\ & \quad \left. + \left(\tilde{A}_\mu^z \right)^2 (1-b)^2(1+b) \right\} C^x(\mathbf{0}), \\ 2 \left[\langle H_{c1}H_{c2}H_{c4} \rangle_{\varphi c} H_{c0} \right]_D &= 2\lambda^2 t_\mu^{-3} \int d^2\mathbf{x} \left\{ \left[\left(\tilde{A}_\mu^x \right)^2 + \left(\tilde{A}_\mu^y \right)^2 \right] b(1+b) \right. \\ & \quad \left. + \left(\tilde{A}_\mu^z \right)^2 2b(b^2-1) \right\} C^x(\mathbf{0}), \\ \left[\langle H_{c2}^2H_{c3} \rangle_{\varphi c} H_{c0} \right]_D &= 4\lambda^2 t_\mu^{-2} t_s^{-1} \int d^2\mathbf{x} \left\{ \left[\left(\tilde{A}_\mu^x \right)^2 + \left(\tilde{A}_\mu^y \right)^2 \right] b \right. \\ & \quad \left. - \left(\tilde{A}_\mu^z \right)^2 2b(1+b) \right\} C^x(\mathbf{0}), \\ - \left[\langle H_1H_{c2}^2H_{c4} \rangle_{\varphi c} H_{c0} \right]_D &= -2\lambda^2 t_\mu^{-2} t_s^{-1} \int d^2\mathbf{x} \left\{ \left[\left(\tilde{A}_\mu^x \right)^2 + \left(\tilde{A}_\mu^y \right)^2 \right] (1+b)(2+b) \right. \\ & \quad \left. + \left(\tilde{A}_\mu^z \right)^2 2(1+b)(1-b)^2 \right\} C^x(\mathbf{0}), \\ \left[\langle H_{c1}H_{c2} \rangle_{\varphi c}^2 \right]_D &= 2\lambda^2 t_\mu^{-2} t_s^{-1} \int d^2\mathbf{x} \left\{ \left[\left(\tilde{A}_\mu^x \right)^2 + \left(\tilde{A}_\mu^y \right)^2 \right] b^2 \right. \end{aligned}$$

$$\begin{aligned}
& + \left(\tilde{A}_\mu^z \right)^2 (2 + t_s t_\mu^{-1}) b^2 \Big\} C^x(\mathbf{0}), \\
\frac{1}{4} \left[\langle H_1 H_{c2}^2 \rangle_{\varphi c} \right]_D &= \lambda^2 t_\mu^{-1} t_s^{-2} \int d^2 \mathbf{x} \left\{ \left[\left(\tilde{A}_\mu^x \right)^2 + \left(\tilde{A}_\mu^y \right)^2 \right] (1 + b)^2 \right. \\
& \quad \left. + \left(\tilde{A}_\mu^z \right)^2 (1 - b)^2 \right\} C^x(\mathbf{0}), \\
- \left[\langle H_1 H_{c2}^2 \rangle_{\varphi c} \langle H_{c1} H_{c2} \rangle_{\varphi c} \right]_D &= -2 \lambda^2 t_\mu^{-2} t_s^{-1} \int d^2 \mathbf{x} \left\{ \left[\left(\tilde{A}_\mu^x \right)^2 + \left(\tilde{A}_\mu^y \right)^2 \right] b(1 + b) \right. \\
& \quad \left. + \left(\tilde{A}_\mu^z \right)^2 2b(b - 1) \right\} C^x(\mathbf{0}).
\end{aligned}$$

The sum of the above terms is (we now again set $t_\mu = t_s$)

$$\begin{aligned}
\lambda t_s^{-2} \int d^2 \mathbf{x} \left\{ \left[\left(\tilde{A}_\mu^x \right)^2 + \left(\tilde{A}_\mu^y \right)^2 \right] \left(1 + \frac{4(b-1)t_s + (b^2-3)\lambda}{t_s} C^x(\mathbf{0}) \right) \right. \\
\left. + \left(\tilde{A}_\mu^z \right)^2 \left((1+b)^2 - \frac{4(1+b)^3 t_s + (3+6b+b^2)\lambda}{t_s} C^x(\mathbf{0}) \right) \right\}. \tag{D13}
\end{aligned}$$

a. On the calculation of disorder terms

As an illustration, we give details for the calculation of the variance terms for a relatively simple term, $\left[\langle H_{c3} \rangle_{\varphi c} H_{c0} \right]_D$, and a more involved one, $\left[\langle H_{c1} H_{c2}^2 H_{c4} \rangle_{\varphi c} H_{c0} \right]_D$. For $\left[\langle H_{c3} \rangle_{\varphi c} H_{c0} \right]_D$ we have

$$\begin{aligned}
\left[\langle H_{c3} \rangle_{\varphi c} H_{c0} \right]_D &= 8 \int d^2 \mathbf{x} d^2 \mathbf{x}' p_{k\mu} p_{k'\mu'} \epsilon_{ijk} \epsilon_{i'j'k'} \epsilon_{abc} \epsilon_{a'b'c'} C^l(\mathbf{0}) \tilde{n}_{j'}^{a'} \tilde{n}_{k'}^{c'} \tilde{A}_{\mu'}^{i'} \times \\
& \quad \left\{ 2\epsilon_{jlm} \epsilon_{klq} \tilde{n}_m^a \tilde{n}_q^c \tilde{A}_\mu^i + 2\epsilon_{ilm} \epsilon_{klq} \tilde{n}_q^c \tilde{n}_j^a \tilde{A}_\mu^m + 2\epsilon_{ilm} \epsilon_{jlq} \tilde{n}_q^a \tilde{n}_k^c \tilde{A}_\mu^m \right. \\
& \quad \left. - \tilde{n}_j^a \tilde{n}_k^c \tilde{A}_\mu^i \left((\epsilon_{ilm})^2 + (\epsilon_{jlm})^2 + (\epsilon_{klm})^2 \right) \right\} \left[Q_\mu^b(\mathbf{x}) Q_{\mu'}^{b'}(\mathbf{x}') \right]_D \\
&= 16\lambda \int d^2 \mathbf{x} p_{k\mu} p_{k'\mu'} \epsilon_{ijk} \epsilon_{i'j'k'} \epsilon_{abc} \epsilon_{a'b'c'} \tilde{n}_{j'}^{a'} \tilde{n}_{k'}^{c'} \tilde{A}_{\mu'}^{i'} \times \\
& \quad \left\{ \left(\epsilon_{jlm} \epsilon_{klq} \tilde{n}_m^a \tilde{n}_q^c \tilde{A}_\mu^i + \epsilon_{ilm} \epsilon_{klq} \tilde{n}_q^c \tilde{n}_j^a \tilde{A}_\mu^m + \epsilon_{ilm} \epsilon_{jlq} \tilde{n}_q^a \tilde{n}_k^c \tilde{A}_\mu^m \right) C^l(\mathbf{0}) \right. \\
& \quad \left. - \tilde{n}_j^a \tilde{n}_k^c \tilde{A}_\mu^i \left(2 + (1+b)^{-1} \right) C^x(\mathbf{0}) \right\} \\
&= 16\lambda \int d^2 \mathbf{x} (\epsilon_{ijk})^2 \left(\tilde{A}_\mu^i \right)^2 \left\{ p_{k\mu} p_{j\mu} C^i(\mathbf{x}) + p_{k\mu}^2 C^i(\mathbf{x}) + p_{k\mu} p_{i\mu} C^j(\mathbf{x}) \right. \\
& \quad \left. + p_{k\mu} p_{i\mu} C^k(\mathbf{x}) + p_{k\mu}^2 C^k(\mathbf{x}) + p_{k\mu} p_{j\mu} C^k(\mathbf{x}) \right. \\
& \quad \left. - \left(2 + (1+b)^{-1} \right) C^x(\mathbf{0}) \left(p_{k\mu}^2 + p_{k\mu} p_{j\mu} \right) \right\}, \tag{D14}
\end{aligned}$$

where we again used the orthonormality of the \mathbf{n}_k . Performing the summation over the silent indices, one finally obtains

$$\begin{aligned}
&= 16\lambda \int d^2 \mathbf{x} \left\{ \left[\left(\tilde{A}_\mu^x \right)^2 + \left(\tilde{A}_\mu^y \right)^2 \right] \left(p_{1\mu}^2 - p_{3\mu}^2 \right) + \left(\tilde{A}_\mu^z \right)^2 \left(4p_{3\mu} p_{1\mu} - 4p_{1\mu}^2 \right) \right\} C^x(\mathbf{0}) \\
&= 4\lambda t_\mu^{-2} \int d^2 \mathbf{x} \left\{ \left[\left(\tilde{A}_\mu^x \right)^2 + \left(\tilde{A}_\mu^y \right)^2 \right] b - \left(\tilde{A}_\mu^z \right)^2 2b(1+b) \right\} C^x(\mathbf{0}).
\end{aligned}$$

We now turn to the more lengthy evaluation of $\left[\langle H_1 H_{c2}^2 H_{c4} \rangle_{\varphi c} H_{c0} \right]_D$. We have

$$\begin{aligned}
H_1 H_{c2}^2 H_{c4} &= 16 \int d^2 \mathbf{x} d^2 \mathbf{x}' d^2 \mathbf{x}'' d^2 \mathbf{x}''' p_{k\mu} t_\mu^{-1} p_{k'\mu'} p_{k''\mu''} p_{k'''\mu'''} \epsilon_{ijk} \epsilon_{i'j'k'} \epsilon_{i''j''k''} \epsilon_{i'''j'''k'''} \times \\
& \quad \epsilon_{abc} \epsilon_{a'b'c'} \epsilon_{a''b''c''} \epsilon_{a'''b'''c'''} \tilde{A}_{\mu'}^{i'} (1 - b\delta_{i'z} + 2b\delta_{j'z}) \tilde{n}_{j'}^{a''} \tilde{n}_{k'}^{c''} \tilde{n}_{j''}^{a'''} \tilde{n}_{k''}^{c'''} \times
\end{aligned}$$

$$\begin{aligned} & \{2\partial_\mu\varphi^i\varphi^d(\epsilon_{kdl}\tilde{n}_l^c\tilde{n}_j^a + \epsilon_{jdl}\tilde{n}_l^a\tilde{n}_k^c) + \varphi^d\partial_\mu\varphi^l\epsilon_{idl}\tilde{n}_j^a\tilde{n}_k^c\} \times \\ & \partial_{\mu'}\varphi^{j'}\varphi^{k'}\partial_{\mu''}\varphi^{i''}\partial_{\mu'''}\varphi^{i'''}Q_\mu^bQ_{\mu''}^{b''}Q_{\mu'''}^{b'''} \end{aligned} \quad (\text{D15})$$

We now need to perform the average over the φ fields. For convenience, we split $H_1H_{c2}^2H_{c4} = \mathcal{A} + \mathcal{B}$ into two terms, where \mathcal{A} corresponds to the part of $H_1H_{c2}^2H_{c4}$ which involves the first term in the curly brackets in Eq. (D15) and \mathcal{B} corresponds to the second term in the curly brackets. For $\langle \mathcal{A} \rangle_{\varphi c}$, we need to calculate the average

$$\left\langle \partial_\mu\varphi^i(\mathbf{x})\varphi^d(\mathbf{x})\partial_{\mu'}\varphi^{j'}(\mathbf{x}')\varphi^{k'}(\mathbf{x}')\partial_{\mu''}\varphi^{i''}(\mathbf{x}'')\partial_{\mu'''}\varphi^{i'''}(\mathbf{x}''') \right\rangle_\varphi, \quad (\text{D16})$$

which can be easily done via Wick's Theorem. However, not all possible permutations of pairings will contribute. All terms involving either of the contractions $\langle id \rangle$ or $\langle j'k' \rangle$ vanish as $\partial_\mu C^x(\mathbf{0}) = 0$. Although not immediately apparent, terms involving the pairing $\langle i''i''' \rangle$ also do not contribute to one loop order. This can be seen only after the computation of the disorder average $\left[\langle \mathcal{A} \rangle_{\varphi c} H_{c0} \right]_D$ and a gradient expansion similar to the one employed below Eq. (D1). Using the same arguments as we used for the term (D1), all $\langle i''i''' \rangle$ contractions can then be shown to give no contribution. Furthermore, all contractions which are identical up to a permutation of the indices i'' and i''' will give the same contributions after the disorder average is taken, as discussed below. We therefore only write down half of the permutations and indicate the others by $\{\mu'' \leftrightarrow \mu'''\}$. Thus, we only need to keep the following terms,

$$\begin{aligned} & \left\langle \partial_\mu\varphi^i(\mathbf{x})\varphi^d(\mathbf{x})\partial_{\mu'}\varphi^{j'}(\mathbf{x}')\varphi^{k'}(\mathbf{x}')\partial_{\mu''}\varphi^{i''}(\mathbf{x}'')\partial_{\mu'''}\varphi^{i'''}(\mathbf{x}''') \right\rangle_\varphi \rightarrow \\ & \delta_{ij'}\delta_{di''}\delta_{k'i'''}\partial_\mu\partial_{\mu'}C^i(\mathbf{x}-\mathbf{x}')\partial_{\mu''}C^d(\mathbf{x}-\mathbf{x}'')\partial_{\mu'''}C^{i'''}(\mathbf{x}'-\mathbf{x}''') \\ & + \delta_{ik'}\delta_{di''}\delta_{j'i'''}\partial_\mu C^i(\mathbf{x}-\mathbf{x}')\partial_{\mu''}C^d(\mathbf{x}-\mathbf{x}'')\partial_{\mu'''}C^{i'''}(\mathbf{x}'-\mathbf{x}''') \\ & + \delta_{ii''}\delta_{dj'}\delta_{k'i'''}\partial_\mu\partial_{\mu'}C^i(\mathbf{x}-\mathbf{x}'')\partial_{\mu''}C^d(\mathbf{x}-\mathbf{x}')\partial_{\mu'''}C^{i'''}(\mathbf{x}'-\mathbf{x}''') \\ & + \delta_{ii''}\delta_{dk'}\delta_{j'i'''}\partial_\mu\partial_{\mu'}C^i(\mathbf{x}-\mathbf{x}'')C^d(\mathbf{x}-\mathbf{x}')\partial_{\mu''}\partial_{\mu'''}C^{i'''}(\mathbf{x}'-\mathbf{x}''') \\ & + \{\mu'' \leftrightarrow \mu'''\} \end{aligned} \quad (\text{D17})$$

Let us now perform the disorder average $\left[\langle \mathcal{A} \rangle_{\varphi c} H_{c0} \right]_D$. For this, we need to calculate

$$\left[Q_\mu^{\tilde{b}}(\tilde{\mathbf{x}})Q_\mu^b(\mathbf{x})Q_{\mu''}^{b''}(\mathbf{x}'')Q_{\mu'''}^{b'''}(\mathbf{x}''') \right]_D \quad (\text{D18})$$

where the variables carrying a tilde arise from the H_{c0} term. Again, we can use Wick's Theorem to decompose the average. Of the three possible permutations of pairings, two involve either of the two contractions $\langle bb'' \rangle$ or $\langle bb''' \rangle$. Neither permutation contributes. This is easily seen for the $\langle bb'' \rangle$ contraction and the explicitly written terms in (D17) because they all involve after the contraction a derivative of $C^x(\mathbf{0})$ and thus vanish. The same terms also do not contribute for the case of a $\langle bb''' \rangle$ contraction, which again can be seen with a gradient expansion and using arguments analogous to those below Eq. (D1). Therefore, only one term of the disorder average must be kept,

$$\left[Q_\mu^{\tilde{b}}(\tilde{\mathbf{x}})Q_\mu^b(\mathbf{x})Q_{\mu''}^{b''}(\mathbf{x}'')Q_{\mu'''}^{b'''}(\mathbf{x}''') \right]_D \rightarrow \lambda^2\delta_{b\tilde{b}}\delta_{b''b'''}\delta_{\mu\tilde{\mu}}\delta_{\mu''\mu'''}\delta(\mathbf{x}-\tilde{\mathbf{x}})\delta(\mathbf{x}''-\mathbf{x}''') \quad (\text{D19})$$

The terms in (D17) which only differ by a permutation of the double primed and triple primed variables give then identical contributions, as such a permutation simply relabels the variables associated with the two H_{c2} terms in $\left[\langle \mathcal{A} \rangle_{\varphi c} H_{c0} \right]_D$. With (D17, D19) we then have

$$\begin{aligned} \left[\langle \mathcal{A} \rangle_{\varphi c} H_{c0} \right]_D &= 128\lambda^2 \int d^2\mathbf{x}d^2\mathbf{x}'d^2\mathbf{x}''t_\mu^{-1} (p_{k''\mu''}^2 + p_{k''\mu''}p_{j''\mu''})^2 (\epsilon_{i''j''k''})^2 \epsilon_{i'j'k'}\tilde{A}_{\mu'}^{i'} \times \\ & (1 - b\delta_{i'z} + 2b\delta_{j'z}) \left\{ -\tilde{A}_{\mu'}^k p_{i\mu}p_{k\mu}\epsilon_{kdi} + \tilde{A}_{\mu'}^k p_{d\mu}p_{k\mu}\epsilon_{idk} - \tilde{A}_{\mu'}^j p_{d\mu}^2 \epsilon_{ij d} \right. \\ & \left. - \tilde{A}_{\mu'}^j p_{i\mu}p_{d\mu}\epsilon_{jdi} \right\} \times \\ & \left[\delta_{ij'}\delta_{di''}\delta_{k'i'''}\partial_\mu\partial_{\mu'}C^i(\mathbf{x}-\mathbf{x}')\partial_{\mu''}C^d(\mathbf{x}-\mathbf{x}'')\partial_{\mu'''}C^{i'''}(\mathbf{x}'-\mathbf{x}''') \right. \\ & + \delta_{ik'}\delta_{di''}\delta_{j'i'''}\partial_\mu C^i(\mathbf{x}-\mathbf{x}')\partial_{\mu''}C^d(\mathbf{x}-\mathbf{x}'')\partial_{\mu'''}C^{i'''}(\mathbf{x}'-\mathbf{x}''') \\ & + \delta_{ii''}\delta_{dj'}\delta_{k'i'''}\partial_\mu\partial_{\mu'}C^i(\mathbf{x}-\mathbf{x}'')\partial_{\mu''}C^d(\mathbf{x}-\mathbf{x}')\partial_{\mu'''}C^{i'''}(\mathbf{x}'-\mathbf{x}''') \\ & \left. + \delta_{ii''}\delta_{dk'}\delta_{j'i'''}\partial_\mu\partial_{\mu'}C^i(\mathbf{x}-\mathbf{x}'')C^d(\mathbf{x}-\mathbf{x}')\partial_{\mu''}\partial_{\mu'''}C^{i'''}(\mathbf{x}'-\mathbf{x}''') \right]. \end{aligned} \quad (\text{D20})$$

The integration over \mathbf{x}'' can now be performed with

$$t_{\mu''}^{-1} \int d^2 \mathbf{x}'' \partial_{\mu''} C^x(\mathbf{x} - \mathbf{x}'') \partial_{\mu''} C^x(\mathbf{x}' - \mathbf{x}'') = \frac{1}{2} C^x(\mathbf{x} - \mathbf{x}') + \mathcal{O}(\kappa^2). \quad (\text{D21})$$

The remaining double integral over \mathbf{x} and \mathbf{x}' can then again be approximated with a gradient expansion in the relative coordinate and employing Eq. (D21). We then obtain (we denote the center of mass coordinate again by \mathbf{x})

$$\begin{aligned} \left[\langle \mathcal{A} \rangle_{\varphi c} H_{c0} \right]_D &\simeq 16\lambda^2 t_s \int d^2 \mathbf{x} (p_{k''}^2 + p_{k''} p_{j''})^2 (\epsilon_{i'' j'' k''})^2 \epsilon_{i' j' k'} \tilde{A}_{\mu}^{i'} (1 - b\delta_{i' z} + 2b\delta_{j' z}) \times \\ &\quad \beta_i \beta_d \epsilon_{idk} \left\{ \tilde{A}_{\mu}^k p_{i\mu} p_{k\mu} + \tilde{A}_{\mu}^k p_{d\mu} p_{k\mu} + \tilde{A}_{\mu}^j p_{d\mu}^2 + \tilde{A}_{\mu}^j p_{i\mu} p_{d\mu} \right\} \times \\ &\quad [\delta_{ij'} \delta_{di''} \delta_{k'i''} \beta_{k'} - \delta_{ik'} \delta_{di''} \delta_{j'i''} \beta_{j'} - \delta_{ii''} \delta_{dj'} \delta_{k'i''} \beta_{k'} + \delta_{ii''} \delta_{dk'} \delta_{j'i''} \beta_{j'}] \times \\ &\quad \times C^x(\mathbf{0}). \end{aligned} \quad (\text{D22})$$

where β_k is defined through $\beta_1 = \beta_2 = 1$, $\beta_3 = (1+b)^{-1}$ and $p_k t_s / t_{\mu} = p_{k\mu}$. After some straightforward algebra, one finally finds

$$\begin{aligned} \left[\langle \mathcal{A} \rangle_{\varphi c} H_{c0} \right]_D &\simeq 32\lambda^2 t_{\mu}^{-2} t_s^3 \int d^2 \mathbf{x} \left\{ \left[\left(\tilde{A}_{\mu}^x \right)^2 + \left(\tilde{A}_{\mu}^y \right)^2 \right] \times \right. \\ &\quad \left. \left((p_1 + p_3)^2 + \frac{4p_1^2}{1+b} \right) \left((p_1 + p_3)^2 + 2p_1^2 + 2p_1 p_3 \right) + \right. \\ &\quad \left. \left(\tilde{A}_{\mu}^z \right)^2 8(1-b) (p_1^2 + p_1 p_3) (p_1 + p_3)^2 \right\} C^x(\mathbf{0}). \end{aligned} \quad (\text{D23})$$

The calculation of $\left[\langle \mathcal{B} \rangle_{\varphi c} H_{c0} \right]_D$ can be done in much the same way as just shown for $\left[\langle \mathcal{A} \rangle_{\varphi c} H_{c0} \right]_D$. One arrives at

$$\begin{aligned} \left[\langle \mathcal{B} \rangle_{\varphi c} H_{c0} \right]_D &\simeq -32\lambda^2 t_{\mu}^{-2} t_s^3 \int d^2 \mathbf{x} \left\{ \left[\left(\tilde{A}_{\mu}^x \right)^2 + \left(\tilde{A}_{\mu}^y \right)^2 \right] \left((p_1 + p_3)^2 + \frac{4p_1^2}{1+b} \right) (p_1 + p_3)^2 \right. \\ &\quad \left. + \left(\tilde{A}_{\mu}^z \right)^2 8(1-b) p_1^2 (p_1 + p_3)^2 \right\} C^x(\mathbf{0}). \end{aligned} \quad (\text{D24})$$

Finally, expressing all p_k through b and t_s , one obtains for $\left[\langle \mathcal{A} + \mathcal{B} \rangle_{\varphi c} H_{c0} \right]_D$

$$\begin{aligned} \left[\langle H_1 H_{c2}^2 H_{c4} \rangle_{\varphi c} H_{c0} \right]_D &= 2\lambda^2 t_{\mu}^{-2} t_s^{-1} \int d^2 \mathbf{x} \left\{ \left[\left(\tilde{A}_{\mu}^x \right)^2 + \left(\tilde{A}_{\mu}^y \right)^2 \right] (1+b)(2+b) \right. \\ &\quad \left. + \left(\tilde{A}_{\mu}^z \right)^2 2(1+b)(1-b)^2 \right\} C^x(\mathbf{0}). \end{aligned} \quad (\text{D25})$$

¹ M.-H. Julien, *Physica B* **329-333**, 693 (2003), and references therein.

² B. I. Shraiman and E. D. Siggia, *Phys. Rev. Lett.* **61**, 467 (1988).

³ B. I. Shraiman and E. D. Siggia, *Phys. Rev. Lett.* **62**, 1564 (1989).

⁴ B. I. Shraiman and E. D. Siggia, *Phys. Rev. B* **40**, 9162 (1989).

⁵ M. Yu. Kuchiev and O. P. Sushkov, *Physica C* **218**, 197 (1993).

⁶ S. Wakimoto *et al.*, *Phys. Rev. B* **67**, 184419 (2003).

⁷ T. Dombre, *J. Phys. (France)* **51**, 847 (1990); A. Auerbach

and B. E. Larson, *Phys. Rev. B* **43** 7800 (1991).

⁸ S. Chakravarty, B. I. Halperin, and D. R. Nelson, *Phys. Rev. B* **39**, 2344 (1989).

⁹ R. J. Birgeneau *et al.*, *Phys. Rev. B* **59**, 13788 (1999).

¹⁰ Ch. Niedermayer *et al.*, *Phys. Rev. Lett.* **80**, 3843 (1998).

¹¹ F. C. Chou *et al.*, *Phys. Rev. Lett.* **71**, 2323 (1993).

¹² F. Borsa *et al.*, *Phys. Rev. B* **52**, 7334 (1995).

¹³ B. Keimer *et al.*, *Phys. Rev. B* **46**, 14034 (1992).

¹⁴ C. Y. Chen *et al.*, *Phys. Rev. B* **51**, 3671 (1995).

¹⁵ S. Wakimoto *et al.*, *Phys. Rev. B* **60**, R769 (1999); *ibid.* **61**, 3699 (2000); S. Wakimoto, S. Ueki, Y. Endoh, and K. Yamada *ibid.* **62**, 3547 (2000).

- ¹⁶ M. Matsuda *et al.*, Phys. Rev. B **61**, 4326 (2000); *ibid.* **62**, 9148 (2000).
- ¹⁷ M. Fujita *et al.*, Phys. Rev. B **65**, 064505 (2002).
- ¹⁸ G. F. Reiter, Phys. Rev. B **49**, R1536 (1994).
- ¹⁹ A. Ramsak and P. Horsch, Phys. Rev. B **57**, 4308 (1998).
- ²⁰ R. J. Gooding, Phys. Rev. Lett. **66**, 2266 (1991).
- ²¹ A. Aharony, R. J. Birgeneau, A. Coniglio, M. A. Kastner, and H. E. Stanley, Phys. Rev. Lett. **60**, 1330 (1988).
- ²² J. Villain, Zeit. f. Phys. B **33**, 31 (1979).
- ²³ L. I. Glazman and A. S. Ioselevich, Zeit. f. Phys. B **80**, 133 (1990).
- ²⁴ V. Cherepanov, I. Y. Korenblit, A. Aharony, and O. Entin-Wohlman, Eur. Phys. J. B **8**, 511 (1999).
- ²⁵ A. N. Lavrov, Y. Ando, S. Komiyama, and I. Tsukada, Phys. Rev. Lett. **87**, 017007 (2001).
- ²⁶ R. J. Gooding, N. M. Salem, and A. Mailhot, Phys. Rev. B **49**, 6067 (1994).
- ²⁷ C. Goldenberg and A. Aharony, Phys. Rev. B **56**, 661 (1997).
- ²⁸ N. Hasselmann, A. H. Castro Neto, and C. Morais Smith, Europhys. Lett. **56**, 870 (2001).
- ²⁹ N. Hasselmann, A. H. Castro Neto, and C. Morais Smith, Phys. Rev. Lett. **82**, 2135 (1999).
- ³⁰ B. P. Stojkovic *et al.*, Phys. Rev. B **62**, 4353 (2000).
- ³¹ P. Azaria, B. Delamotte, F. Delduc, and T. Jolicoeur, Nucl. Phys. B **408**, 485 (1993).
- ³² S. Klee and A. Muramatsu, Nucl. Phys. B **473**, 539 (1996).
- ³³ T. Dombre and N. Read, Phys. Rev. B **39**, 6797 (1989).
- ³⁴ J. A. Hertz, Phys. Rev. B **18**, 4875 (1978).
- ³⁵ W. Apel, M. Wintel, and H. U. Everts, Zeit. f. Phys. B **86**, 139 (1992).
- ³⁶ K. Binder and A. P. Young, Rev. Mod. Phys. **58**, 801 (1986).
- ³⁷ A. M. Polyakov, Phys. Lett. **59 B**, 79 (1975).
- ³⁸ Y. Imry and S. K. Ma, Phys. Rev. Lett. **35**, 1399 (1975).
- ³⁹ M. Wintel, H. U. Everts, and W. Apel, Europhys. Lett. **25**, 711 (1994).
- ⁴⁰ J. M. Kosterlitz and D. J. Thouless, J. Phys. C **6**, L97 (1973).
- ⁴¹ H. Kawamura, J. Phys.:Condens. Matter **10**, 4707 (1998).
- ⁴² M. Wintel, H. U. Everts, and W. Apel, Phys. Rev. B **52**, 13480 (1995).
- ⁴³ M. Wintel, PhD Thesis, Univ. Hannover 93U7008 (1993).
- ⁴⁴ S. Scheidl, Phys. Rev. B **55**, 457 (1997).
- ⁴⁵ D. S. Fisher, Phys. Rev. B **31**, 7233 (1985).
- ⁴⁶ T. Nattermann, S. Scheidl, S. E. Korshunov, and Mai Suan Li, J. Phys. I France **5**, 565 (1995).
- ⁴⁷ M.-C. Cha and H. A. Fertig, Phys. Rev. Lett. **74**, 4867 (1995).
- ⁴⁸ B. W. Southern and A. P. Young, Phys. Rev. B **48**, 13170 (1993).
- ⁴⁹ B. W. Southern and H.-J. Xu, Phys. Rev. B **52**, R3836 (1995).
- ⁵⁰ O. P. Vajk, P. K. Mang, M. Greven, P. M. Gehring, and J. W. Lynn, Science **295**, 1691 (2002); O. P. Vajk, M. Greven, P. K. Mang, and J. W. Lynn, Sol. St. Comm. **126**, 93 (2003).
- ⁵¹ M. Hücker *et al.*, Phys. Rev. B **59**, R725 (1999).
- ⁵² I. Y. Korenblit, A. Aharony, and O. Entin-Wohlman, Phys. Rev. B **60**, R15017 (1999).
- ⁵³ K. Hirota, K. Yamada, I. Tanaka, and H. Kojima, Physica B **241-243**, 817 (1998).
- ⁵⁴ K. Yamada *et al.*, Phys. Rev. B **57**, 6165 (1998).
- ⁵⁵ H. Kimura *et al.*, Phys. Rev. B **59**, 6517 (1999).
- ⁵⁶ C. Morais Smith, N. Hasselmann, and A. H. Castro Neto, Am. Instit. of Physics Conf. Proc., **554**, 209 (2001).
- ⁵⁷ T. Sasagawa, P. K. Mang, O. P. Vajk, A. Kapitulnik, and M. Greven, Phys. Rev. B **66**, 184512 (2002).
- ⁵⁸ W. Bao, Y. Chen, Y. Qiu, and J. L. Sarrao, Phys. Rev. Lett. **91**, 127005 (2003); W. Bao *et al.*, *ibid.* **84**, 3978 (2000).